

Cosmological Perturbation Theory and the Spherical Collapse model: Part I. Gaussian initial conditions.

Pablo Fosalba and Enrique Gaztañaga

*Institut d'Estudis Espacials de Catalunya, Research Unit (CSIC),
Edf. Nexus-104 - c/ Gran Capità 2-4, 08034 Barcelona, Spain*

5 February 2020

ABSTRACT

We present a simple and intuitive approximation for solving perturbation theory (PT) of small cosmic fluctuations. We consider only the spherically symmetric or monopole contribution to the PT integrals, which yields the exact result for tree-graphs. We find that the non-linear evolution is then given by a *local* transformation over the initial conditions. In the case of gravitational evolution of density fluctuations, this transformation is found to be the spherical collapse (SC) dynamics, as it is the exact solution in the shearless (and therefore local) approximation in Lagrangian space. Taking advantage of this property, it is straightforward to derive the one-point cumulants, ξ_J , for both the unsmoothed and smoothed density fields to *arbitrary* order in the perturbative regime. To leading order this reproduces, and provides with a simple explanation for, the exact results obtained by Bernardeau (1992, 1994). We then show that the SC model leads to accurate estimates for the next corrective terms when compared to the results derived in the exact PT making use of the loop calculations (Scoccimarro & Frieman 1996). The agreement is within a few per cent for the hierarchical ratios $S_J = \xi_J/\xi_2^{J-1}$. We compare our analytic results to N-body simulations, which turn out to be in very good agreement up to scales where $\sigma \approx 1$. A similar treatment is presented to estimate higher order corrections in the Zel'dovich approximation. These results represent a powerful and easy-to-use tool to produce analytical predictions for the cosmological fields in the weakly non-linear regime. A generalisation of the current approach to non-Gaussian initial conditions and non-flat FRW universes will be provided in two accompanying papers (Papers II and III).

1 INTRODUCTION

The probability distribution function contains all the statistical information concerning the cosmic fields: density δ and velocity v fluctuations. Here we will concentrate on its moments, the variance, skewness, kurtosis and so on. For a given set of moments in the initial conditions (IC), we would like to derive the final moments using the exact dynamics that rule the evolution of the underlying field. The problem is that the exact solution to the dynamical equations is only known for the linear regime of the evolution of these fields and only approximate solutions are known for their corresponding non-linear stages.

Perturbation theory (PT) provides a framework to study small departures from linear theory: the weakly non-linear regime. The leading order contribution to the skewness for Gaussian initial conditions (GIC) was obtained by Peebles 1980. Fry 1984 extended this result to higher order moments and Bernardeau 1992 (hereafter B92) found the generating function to the leading order contribution: the tree-level solution.

Comparison with observations and simulations made

it necessary to develop PT for the smoothed fields. The smoothing corrections to the unsmoothed amplitudes for a power-law were first computed for the skewness for either a top-hat or a Gaussian window function by Juskiewicz et al. 1993. For a top-hat filter, Bernardeau 1994a (hereafter B94a) developed the machinery to systematically derive the smoothed hierarchical amplitudes for either the density (S_J) or the velocity divergence (T_J) fields to an arbitrary order (and arbitrary power spectrum). These results were in excellent agreement with numerical simulations (e.g. Baugh, Gaztañaga, Efstathiou 1995, hereafter BGE95; Gaztañaga & Baugh 1995, Colombe et al. 1996). Work by Matsubara 1994 and Lokas et al. 1995 include some results for the Gaussian-smoothed density and velocity cumulants.

The success of the PT approach made it plausible to go further and study higher order (loop) corrections and the case of non-Gaussian initial conditions (NGIC). Despite the impressive achievements in the diagrammatic approach to loop corrections by Scoccimarro & Frieman 1996a and 1996b, (hereafter SF97a and SF97b, respectively), the analytic entanglement faced when carrying out the calculations for the smoothed one-point cumulants is enormous. More-

over, regularization techniques must be used to evaluate the loop corrections through the kernels in Fourier space which, for the values of the spectral index $n \geq -1$ lead to logarithmic divergences which depend on the cut-off used in the regularization. The latter puts constraints on the domain of applicability of the diagrammatic approach. When it comes to calculating the statistics of the smoothed fields, further analytic entanglement makes comparison with simulations and observations be restricted to few discrete values of the spectral index (Scoccimarro 1997, hereafter S97). For NGIC we have to face similar problems to start with, as loop corrections could enter at the same order than the tree-level contribution.

The general results derived by Bernardeau (B92, B94a and Bernardeau 1994b, hereafter B94b) show that the generating function follows the equation for the spherical collapse model. In this context this remarkable result lacked a satisfactory interpretation. What is the connection between PT and the spherical collapse model? Why does the generating functional follow an equation for a fluctuating field? Why is the smoothed generating functional given by the same unsmoothed result but with a different argument? Is this related to the Gaussian nature of the IC or the flatness of space? In this paper we will present a simple interpretation for these results, which will allow us to extend it to higher order corrections and non-Gaussian initial conditions (NGIC).

This paper is organized as follows. In section §2 we give a brief account of perturbation theory (PT). In section §3 we investigate the spherical collapse model and its relation to PT. In section §4 we present a comparison of the SC model with exact PT and N-body Simulations. Further results are derived for the Zel'dovich approximation in section §5.

2 PERTURBATION THEORY AND OTHER APPROXIMATIONS

We will now review briefly the main features of perturbation theory (PT), showing the connection between the tree-graphs in the diagrammatic approach to the one-point statistics and the *monopole* contribution to the kernels. The latter will allow us to use a simple local non-linear transformation (what we shall call the *local-density* transformation) to derive the predictions for the cumulants in the perturbative regime from the *monopole* contribution alone. Throughout this paper we shall focus on GIC and the Einstein-deSitter scenario to gain simplicity. However, a generalisation of the current approach to NGIC and non-flat FRW universes will be provided in two accompanying papers (see Gaztañaga & Fosalba, Fosalba & Gaztañaga 1997, hereafeter Papers II & III).

2.1 Perturbation theory

A convenient approach to solve the field equations is to expand the density contrast δ assuming it is small as is usually done in the context of perturbation theory (PT) in Euler space,

$$\delta(\mathbf{x}, t) = \delta_1(\mathbf{x}, t) + \delta_2(\mathbf{x}, t) + \delta_3(\mathbf{x}, t) \dots, \quad (1)$$

where we assume that $\delta_n \ll \delta_{n-1}$. The first term $\delta_1 \equiv \delta$ is the solution to the linearized field equations and is given in terms of the linear growth factor $D(t)$. The second term $\delta_2 \sim \delta_l^2$ is the second-order solution, obtained by using the linear solution in the source terms, and so on.

The dominant mode to the linear PT solution, δ_l , is given in terms of the linear growth factor $D(t): \delta_l(x, t) = D(t) \delta(x, 0)$, which for $\Omega = 1$, the so-called Einstein-deSitter universe, gives $D(t) = a(t)$. The linear approximation is therefore trivially local: *the evolution of a density fluctuation at a given point is not affected by its neighbouring density fluctuations*, and all fluctuations grow with time at the same rate.

Beyond linear order, the equations of motion can be integrated for an Einstein-de Sitter universe, yielding for the growing mode (Peebles 1980),

$$\delta_2 = \frac{5}{7} \delta_l^2 + \delta_{l,\alpha} \Delta_{,\alpha} + \frac{2}{7} \Delta_{,\alpha\beta} \Delta_{,\alpha\beta} \quad (2)$$

where $_{,\alpha}$ are partial space derivatives and we denote, $\Delta(\mathbf{x}) = -4\pi \int d^3 \mathbf{x}' \delta(\mathbf{x}') / |\mathbf{x} - \mathbf{x}'|$.

The second order solution Eq.[2], explicitly shows that, although δ_2 is of order δ_l^2 , PT is formally *non-local* already at the second order as explicitly realised by the term accounting for the potential generated by the density fluctuations at different points ($\sim \Delta$). In fact, the non-local nature of gravity is an intrinsic feature of General Relativity and remains so in the Newtonian limit through the tidal forces when the appropriate limit to the equations of motion is taken as was recently shown by Kofman & Pogosyan 1995.

To win simplicity in the equations of motion it is convenient to work in Fourier space:

$$\delta(\mathbf{k}) \equiv \frac{1}{V} \int d^3 x \delta(\mathbf{x}) \exp(i\mathbf{k} \cdot \mathbf{x}) \quad (3)$$

So that one can formally write, $\delta(\mathbf{k}) \equiv \sum_{n=1}^{\infty} \delta_n(\mathbf{k})$, being $\delta_n(\mathbf{k})$ the n -th order perturbative contribution. The latter is expressed as an n -dimensional integral over the kernels, F_n , that encode the nonlinear coupling of modes due to the gravitational evolution,

$$\begin{aligned} \delta_n(\mathbf{k}) &= \int d^3 q_1 \dots d^3 q_n \delta_D(\mathbf{k} - \mathbf{q}_1 \dots - \mathbf{q}_n) \times \\ &\times F_n(\mathbf{q}_1 \dots \mathbf{q}_n) \delta_1(\mathbf{q}_1) \dots \delta_1(\mathbf{q}_n) \end{aligned} \quad (4)$$

where δ_D is the Dirac function and the kernels F_n are given by symmetric homogeneous functions of \mathbf{q}_n with degree zero, that is, some geometrical average (see Fry 1984, Goroff et al. 1986, Jain & Bertschinger 1994, SF96a). In particular, for the second order we have:

$$F_2(\mathbf{q}_1, \mathbf{q}_2) = \frac{5}{7} + \frac{1}{2} \frac{\mathbf{q}_1 \cdot \mathbf{q}_2}{q_1 q_2} \left(\frac{q_1}{q_2} + \frac{q_2}{q_1} \right) + \frac{2}{7} \left(\frac{\mathbf{q}_1 \cdot \mathbf{q}_2}{q_1 q_2} \right)^2 \quad (5)$$

which reproduces Eq.[2] in Fourier space.

2.2 Statistical Properties

These perturbative solutions can be used to study the evolved statistical properties of the density fluctuations, which is our final goal. Here we concentrate on the J -order moments of the fluctuating field: $m_J \equiv \langle \delta^J \rangle$. In this notation the variance is defined as:

$$Var(\delta) \equiv \sigma^2 \equiv m_2 - m_1^2 \quad (6)$$

In general, it is interesting to introduce the *connected moments* ξ_J , which carry statistical information independent of the lower order moments, and are formally denoted by a bracket with subscript c :

$$\xi_J \equiv \langle \delta^J \rangle_c \quad (7)$$

The connected moments are also called *cumulants*, *reduced moments* or *irreducible moments*. For a Gaussian distribution $\xi_J = 0$ for $J > 2$. In many cases the higher order cumulants of a particular distribution are given in terms of the second order one ξ_2 . It is therefore convenient to introduce some more definitions. A *dimensional scaling* of the higher order moments in terms of the second order one $\xi_2 = \sigma^2$ is given by the following ratios:

$$B_J \equiv \frac{\xi_J}{\sigma^J} = \frac{\xi_J}{\xi_2^{J/2}} \quad (8)$$

We will see that for GIC in perturbation theory, it is more useful to introduce the *hierarchical coefficients*,

$$S_J = \frac{\xi_J}{\xi_2^{J-1}}, \quad (9)$$

as PT predicts these quantities to be time-independent quantities on large scales. These amplitudes are also called normalized one-point cumulants or reduced cumulants. We shall also use *skewness*, for S_3 and *kurtosis*, for S_4 .

The way to proceed is to substitute the PT calculations Eq.[4] and commute the spatial integrals in δ_n with the expectation values $\langle \dots \rangle$, by using the *fair sample hypothesis* (§30 Peebles 1980). Thus the calculation will reduce to averages over moments of δ_1 with the kernels in Eq.[4], which will, in turn, give us the statistical properties of δ in term of the ones in the IC.

2.3 Linear Theory

If we only consider the first term in the PT series, Eq.[1], and the growing mode, the cumulants of the evolved field will just be, $\langle \delta^J \rangle_c = D^J \langle \delta_0^J \rangle_c$, were $\langle \delta_0^J \rangle_c$ correspond to the cumulants in the IC. Consistently, the hierarchical ratios (see Eq.[9]) will scale as, $S_J = S_J(0)/D^{J-2}$, were $S_J(0)$ are the initial ratios. Note that this implies that the linear growth erases the initial hierarchical ratios, so that $S_J \rightarrow 0$, as time evolves (and $D \rightarrow \infty$).

In terms of the dimensional scaling, see Eq.[8], we have, $B_J = B_J(0)$, so that the linear growth preserves the initial values. Note that if we want to do a meaningful calculation of these ratios or the cumulants, in general, we might need to consider more terms in the perturbation series, Eq.[1], depending on the statistical properties of the IC, e.g. how they scale with the initial variance, which is typically the smallness parameter in the expansion of the cumulants.

For GIC both $B_J(0) = S_J(0) = 0$, and we have to consider higher order terms in the perturbation series to be able to make a non-vanishing prediction.

2.4 The tree-level

The computation of the cumulants in PT dates back to Peebles (1980) work where the leading order contribution to the

skewness was obtained making use of the second-order PT as given in Eq.[2] to give,

$$S_3 \equiv \frac{\langle \delta^3 \rangle_c}{\langle \delta^2 \rangle^2} = \frac{34}{7} + \mathcal{O}[\sigma_1^2]. \quad (10)$$

Fry 1984 extended Peebles analysis by making the connection between tree diagrams (or tree-graphs) and the perturbative contributions to leading order in the GIC case. With the help of this formalism he was able to obtain the leading order contributions for the three- and four-point functions making use of the 2nd. and 3rd. order in PT. Later on, Bernardeau 1992 found the generating function of the one-point cumulants to leading order for GIC. Furthermore, Fry found in general that the lowest order (tree-level) connected part that contributes to ξ_J are of order $2(J-1)$ in δ_1 from terms like:

$$\langle \delta_1^2 \delta_2^{J-2} \rangle + \dots + \langle \delta_1^{J-1} \delta_{J-1} \rangle. \quad (11)$$

Note that this involves the cancellation of $J-2$ contribution to the moment of order J , m_J . This is a property of the GIC for which all $\langle \delta_1^J \rangle_c$ vanish for $J > 2$.

The above result Eq.[11] can be understood as follows. We are only interested in estimating the leading order contribution (in terms of δ_1) to the connected part of the expectation value of the product $\delta_1 \delta_2 \dots \delta_n$, e.g. made with terms that can not be factorized as products containing disjoint subsets of the labels. Each δ is to be replaced with the perturbative expansion (see Eq.[1]), so that it may contain an arbitrary power in δ_1 . In the GIC case, the moments factorized only by pairs, so that the smaller contribution, with the smaller number of δ_1 , connecting J points has $J-1$ pairs. Each pair corresponds to two δ_1 and therefore the leading contribution has indeed $2(J-1)$ terms. These are the tree diagrams, corresponding to graphs with no loops (as any graph involving loops implies higher orders in δ_1).

2.5 The local nature of the tree-level: the monopole approximation

Consider a generic term of a tree-level contribution such as $\langle \delta_n(k_1) \delta_1(k_2) \dots \delta_1(k_{n-1}) \rangle$. From Eq.[4] we have:

$$\begin{aligned} \langle \delta_n(k_1) \delta_1(k_2) \dots \delta_1(k_{n-1}) \rangle &= \int d^3 q_1 \dots d^3 q_n \times \\ &\times \delta_D(k_1 - q_1 \dots - q_n) F_n(q_1 \dots q_n) \times \\ &\times \langle \delta_1(q_1) \dots \delta_1(q_n) \delta_1(k_2) \dots \delta_1(k_{n-1}) \rangle \end{aligned} \quad (12)$$

So we only have to perform the spatial integral over the initial moments $\langle \delta_1^{2(n-1)} \rangle$. In the case of GIC these moments are just products of two-point functions. The only terms in the products of two-point functions that produce *connected* graphs have pairs connected like:

$$\begin{aligned} \int d^3 q_1 \dots d^3 q_n \delta_D(k_1 - q_1 \dots - q_n) F_n(q_1 \dots q_n) \\ \langle \delta_1(q_1) \delta_1(k_2) \rangle \langle \delta_1(q_2) \delta_1(k_3) \rangle \dots \langle \delta_1(q_n) \delta_1(k_{n-1}) \rangle, \end{aligned} \quad (13)$$

e.g. those terms with pairs of \mathbf{q} and \mathbf{k} , as otherwise there is a part of the integral that factorizes. By isotropy, one sees that the only dependence in the angles between the \mathbf{q} 's comes through $F_n(q_1 \dots q_n)$. Thus, the geometrical dependence in

Eq.[14] can be integrated out and the contribution of the kernels F_n just become numbers. These numbers are given by the *monopole* term in an expansion of the kernels in spherical harmonics as they correspond to their angle averages (the outcome of the angular integrals in Eq.[14]). In other words, if we decompose the kernels, F_n in multipoles,

$$F_n(\mathbf{k}_1, \dots, \mathbf{k}_n) = F_n^{l=0} + \sum_{l=1}^{\infty} F_n^l, \quad (14)$$

only the first term $F_n^{l=0}$, the *monopole* (angle average of F_n) which is the *spherically symmetric* contribution to the kernels, contributes to the GIC tree-level. We shall define, for convenience, the *monopole* in terms of some numbers ν_n in the way,

$$F_n^{l=0} \equiv \langle F_n \rangle = \nu_n / n!, \quad (15)$$

where the $n!$ reflects the fact that we are looking for some symmetric amplitudes. For instance, from Eq.[5] we have:

$$F_2^{l=0} \equiv \langle F_2 \rangle = \nu_2 / 2! = 34/21. \quad (16)$$

On the other hand, we can write the density fluctuation as formed of some generic *local* and *non-local* components,

$$\delta(\mathbf{x}) \equiv \delta^{loc}(\mathbf{x}) + \delta^{nloc}(\mathbf{x}) \quad (17)$$

where *local* means that the evolved (non-linear) density contrast at a given point is a transformation of the linear density contrast at the same point, what we shall call a *local-density* transformation, $\delta^{loc}(\mathbf{x}) = \mathcal{L}[\delta_1(\mathbf{x})]$. The *non-local* component gives the contribution from density fluctuations at any other points. The latter is non-vanishing at all orders beyond the second in PT as commented above (see §2.1) as gravity is essentially a non-local interaction. The equivalent to this *local-density* transformation in Fourier space would then be, $\delta_{loc}(\mathbf{k}) = \mathcal{L}[\delta_1(\mathbf{k})]$. In particular, we can write the n -th perturbative order of $\delta_{loc}(\mathbf{k})$ in the following way,

$$\delta_n^{loc}(\mathbf{k}) = \frac{c_n}{n!} \delta_1(\mathbf{k}) * \dots * \delta_1(\mathbf{k}) \quad (18)$$

which involves n convolutions of $\delta_1(\mathbf{k})$. By substituting F_n by its monopole contribution, $\nu_n / n!$, in Eq.[4], we immediately see that the above c_n numbers are just those given by the *monopole* term, i.e., $c_n = \nu_n$. Transforming back to real space, we find $\delta_n^{loc}(\mathbf{x}) = c_n / n! [\delta_1(\mathbf{x})]^n$, and thus that the (*Gaussian*) tree-level is given by the *local contribution* to the density fluctuation and has the form,

$$\delta^{loc}(\mathbf{x}) \equiv \sum_{n=1}^{\infty} \delta_n^{loc}(\mathbf{x}) = \mathcal{L}[\delta_1(\mathbf{x})] = \sum_{n=1}^{\infty} \frac{c_n}{n!} [\delta_1(\mathbf{x})]^n, \quad (19)$$

with $c = 1$, to reproduce the linear solution, and $c_n = \nu_n$ to recover the exact tree-level.

As a result, in this scheme, the higher-order multipoles in the kernels are only expected to yield a non-vanishing contribution in the next-to-leading orders (loops) in the cumulants, while the monopole contributes to all perturbative orders. In what follows we shall deal with the *local* contribution to the density fluctuation alone, δ_{loc} (monopole in the kernels) and work out its 1-point statistics.

2.6 Estimation of the cumulants

We can now easily estimate *all* the 1-point statistical properties in the *monopole* approximation to PT. This can be done by using the generating function method:

$$\xi_J = \langle \delta^J \rangle_c = \frac{d^J}{dt^J} \ln \langle e^{t\delta} \rangle |_{t=0}, \quad (20)$$

where the field $\delta \equiv \delta_{loc}$ is given by Eq.[19]. The resulting expressions can be found in FG93, who consider a generic local transformation to find, to leading terms in σ_l :

$$\begin{aligned} S_3 &= 3c_2 + \mathcal{O}(\sigma_l^2) \\ S_4 &= 4c_3 + 12c_2^2 + \mathcal{O}(\sigma_l^2) \\ S_5 &= 5c_4 + 60c_3c_2 + 60c_2^3 + \mathcal{O}(\sigma_l^2) \end{aligned} \quad (21)$$

for GIC. Note that the leading contribution to S_J is enough to specify all the coefficients c_n in the transformation, and therefore all higher order corrections. As expected, by substituting c_2 by the monopole contribution: $c_2 = \nu_2$ in Eq.[16], one recovers Peebles 1980 calculation (10).

2.7 The local-density approximation and the equations of motion.

We shall stress that the local-density transformation (see Eq.[19]) is just a particular case of what is usually understood as *local*. In general, it means that the value of the evolved field at a given point is a transformation of the IC at the same point, say, the initial value of the field, its derivatives and any other fields (e.g. velocity) contributing at that very point. Although gravity is non-local, the results above show that the statistical average of the non-local integrals involved in the reduced moments to leading order are exactly given by a *local-density* transformation.

Note that this argument is true for any dynamics, not only for gravity, it applies to any leading order calculation. But to estimate the leading order (tree-level) it is not necessary to calculate the full kernels F_n , as we only need the c_n numbers, the *monopole* (spherically symmetric) contribution. Therefore, *the values of c_n (and thus the appropriate local-density transformation) can be determined by finding the spherically symmetric solution to the equations of motion*. We shall see below that for gravity this transformation is the spherical collapse (SC), whereas for the ZA, it is what we shall call the Spherically Symmetric ZA (SSZA).

2.8 Other approximations

In one dimension, the probability distribution function of the matter field may be integrated in Lagrangian coordinates making use of the Zel'dovich Approximation (ZA) which recovers the exact dynamics. For the three-dimensional case however, the ZA fails to describe the exact picture since the displacement field (that only depends on the IC) no longer factorizes in the actual solution for the growing mode as the ZA assumes (Bernardeau & Kofman 1995).

In the context of Lagrangian space and inspired by the successful results of the Zel'dovich Approximation (hereafter ZA), there have appeared in the last years a number of local approximations to the exact dynamics that successfully

described the evolution of the density contrast in its first non-linear stages (see Bertschinger and Jain 1994, Hui and Bertschinger 1996). Most recently, Protogeros and Scherrer 1997 (hereafter PS97), following the formalism of the ZA, made use of a closed analytic expression,

$$\delta = (1 - \delta_l/\alpha)^{-\alpha} - 1, \quad (22)$$

to derive the cumulants following the formal analogy between the density contrast and the vertex generating function at tree level (see B92), for different values of α , which they take to be different approximations to the exact PT. For the particular case when $\alpha = 3$ (what they call the “spherical approximation”) their approximation happens to be equal to the spherically symmetric dynamics (in 3 dimensions) for the ZA (what we call SSZA in section 5). They also consider the case $\alpha = 3/2$ as another approximation they call the “exact approximation” (which, in fact, only reproduces the exact tree-level when $\Omega = 0$, see Paper III). In general, none of these local approximations recovers the exact tree-level amplitudes as predicted in PT (which we will show later that it is given by the spherical collapse).

On the other hand, a number of non-local approximations to the non-linear dynamics of the cosmological fields have been designed as to simplify the equations of motion through different assumptions about the corresponding fields. For example: the Linear (or Frozen) Potential Approximation (LPA) which assumes that the gravitational potential generated by the density perturbations remains linear throughout the evolution (see Brainerd et al. 1993, Bagla and Padmanabhan 1994); The Frozen Flow Approximation (FFA) that takes the velocity field to be frozen to its initial shape, $\partial u/\partial a = 0$ (see Matarrese et al. 1992); or the ZA, which deals with the approximation that the particles move on straight lines in the comoving picture (see Zel'dovich 1970). A general treatment in terms of the vertex generating function can be found in Munshi et al. 1994. For a review of all these approximations see Bernardeau et al. 1994. If we write the second perturbative order as given by Eq.[2] in the generic form:

$$\delta = \delta_l + A \delta_l^2 + B \delta_{l,\alpha} \Delta_{,\alpha} + C \Delta_{,\alpha\beta} \Delta_{,\alpha\beta}, \quad (23)$$

one may derive the skewness at tree-level in the parametric fashion,

$$S_3 = 9A - 3B + 5C. \quad (24)$$

In this notation, PT gives $A = 5/7$, $B = 1$, $C = 2/7$, while the ZA yields $1/2$, 1 , $1/2$, whereas the FFA gives $1/2$, $1/2$, 0 , and the LPA gets $1/2$, $7/10$, $1/5$. By just replacing the numbers in S_3 one sees that none of these non-linear approximations is able to reproduce the exact tree-level amplitude given by PT for the skewness. Therefore, despite successfully describing the first non-linear stages of the gravitational collapse of a density fluctuation, none of the above given approximations yields to accurate enough statistical predictions concerning the one-point cumulants in the perturbative regime.

2.9 Higher perturbative orders in PT

Whenever $\delta \lesssim 1$, corrective terms beyond leading order (tree-level) become quantitatively important and must be taken into account. A systematic approach for deriving the

next-to-leading orders in PT was introduced by Goroff et al. 1986 by representing them in terms of the *loop* diagrams. Recently, the first results for the *loop* corrections in PT have been calculated (see SF97a, SF97b and S97).

The angle averaged (spherically symmetric) picture described above can be used to estimate the *monopole* contribution to an arbitrary higher-order in PT. This is easy to do as one just has to take more terms in the series given by Eq.[19] to calculate the next orders in the moments. As expected, even in the GIC case, the higher-order terms coming from the monopole contribution differ from the exact PT estimates. This is because the exact integrations in this case, e.g. such as that in Eq.[12] with more δ_l factors, involve loops and the geometrical dependence is not trivial anymore (the dipole, quadrupole... contributions no longer cancel); The kernel F_n integration will give a different number depending on the loop configuration (see SF97a), contrary to the monopole approximation (where F_n is always replaced by the same amplitude $c_n/n!$). However, one can naively expect that the monopole contribution dominates in all perturbative orders since asymmetric contributions should partially cancel and yield a subdominant contribution in angle-averaged quantities such as the one-point cumulants. In this paper, we shall compute the monopole contribution to PT and will compare it to the exact analytic results, when available, or N-body simulations to see how accurate this approximation is.

3 THE SPHERICAL COLLAPSE (SC) MODEL

3.1 The SC and shearless approximation

We next want to derive the evolution of a density fluctuation within the spherical model of collapse. In order to do that, we turn to the Lagrangian space which is the natural framework for describing the motion of a fluid element. The SC dynamics is fully described in terms of one parameter, the initial size of the spherical fluctuation. In this sense, the SC model is just a particular case within the family of *local-density* approximations discussed above. When we write the equations in Lagrangian space, the natural variable is the density contrast and the only parameter in terms of which the solution is given is the initial (linear) density contrast.

We first must define the conformal time τ which is the comoving time parameter to the motion of the mass and we shall denote with a dot the associated time derivatives (conformal time derivatives), defined as,

$$\frac{d}{d\tau} = \frac{\partial}{\partial\tau} + \mathbf{v} \cdot \nabla_q \equiv a(t) \frac{d}{dt}, \quad (25)$$

$a(t)$ being the scale factor for an Einstein-deSitter universe. The generic equation describing the evolution of a spherically symmetric perturbation in an expanding universe is given by,

$$\frac{d^2R}{dt^2} = -\frac{GM(R)}{R^2} = -4\pi G\rho R \quad (26)$$

since the matter contained in a spherical perturbation of radius R is, $M(R) = 4\pi\rho R^3/3$. Therefore the spherical density perturbation $\delta = (R/a(t)R_0)^{-3} - 1$, is described by the following equation of motion

$$\ddot{\delta} + \mathcal{H}(\tau) \delta - \frac{\Delta}{\exists} \frac{\delta^\epsilon}{(\infty + \delta)} = \Delta \pi \mathcal{G}(\rho - \bar{\rho}) \dot{\tau}^\epsilon (\infty + \delta). \quad (27)$$

where the dot denotes a conformal time derivative, and $a(\tau)$ is the scale factor in terms of the conformal time from which we define the conformal Hubble parameter $\mathcal{H}(\tau) = [\log \dot{\tau}]/[\tau]$. In terms of the comoving time derivative, $d/dt \equiv \cdot$, the latter equation translates into,

$$\ddot{\delta} + 2H(t)\dot{\delta} - \frac{4}{3} \frac{\dot{\delta}^2}{(1 + \delta)} = 4\pi G \bar{\rho} \delta (1 + \delta). \quad (28)$$

where $H(t) = d \log a(t)/dt$.

On the other hand, the Newtonian Fluid equations with zero pressure, which are the appropriate description for the sub-horizon modes in a perturbed FRW universe, in its matter dominated regime (the relevant for describing the collapse of structures), are usually given in Euler space (e.g. Peebles 1980). If we now turn to *Lagrangian* coordinates and we reexpress the equations of motion in terms of the derivatives of the conformal time τ , the continuity equation reads,

$$\dot{\delta} + (1 + \delta) \theta = 0, \quad \theta \equiv \nabla \cdot \mathbf{v}. \quad (29)$$

We then combine the latter with the Raychaudhuri equation,

$$\dot{\theta} + \mathcal{H}(\tau) \theta + \frac{\infty}{\exists} \theta^\epsilon + \sigma^j \sigma_{j|} - \epsilon \omega^\epsilon = -\Delta \pi \mathcal{G} \bar{\rho} \delta \dot{\tau}^\epsilon \quad (30)$$

where $\omega^2 \equiv \frac{1}{2} \omega^{ij} \omega_{ij}$, and the expansion θ , vorticity ω_{ij} , and shear σ_{ij} , are given by the trace, traceless antisymmetric and symmetric parts respectively, of the velocity divergence,

$$\begin{aligned} \nabla_i v_j &= \frac{1}{3} \theta \delta_{ij} + \sigma_{ij} + \omega_{ij}, \\ \sigma_{ij} &= \sigma_{ji}, \quad \omega_{ij} = -\omega_{ji}, \end{aligned} \quad (31)$$

and get a second-order differential equation for the density contrast,

$$\begin{aligned} \ddot{\delta} + \mathcal{H}(\tau) \delta - \frac{\Delta}{\exists} \frac{\delta^\epsilon}{(\infty + \delta)} &= \\ = (1 + \delta) (\sigma^{ij} \sigma_{ij} - 2\omega^2 + 4\pi G \bar{\rho} \delta a^2). \end{aligned} \quad (32)$$

For an initially irrotational fluid (the expansion preserving its irrotational character in the first evolutionary stages): $\omega = 0$. Making the further assumption that there is *no shear*, Eq.[32] leads to the equation we obtained for the SC model (see Eq.[27] above). In other words, *the SC approximation is the actual dynamics when the tidal effects are neglected*. As one would expect, this yields a local dynamics, where the evolved field at a point is just given by a local (non-linear) transformation of the initial field at the same point. Throughout this paper we shall drop the shear term and work out the exact solution for this dynamics in the perturbative regime.

The exact (non-perturbative) solution for the SC of the density contrast in an Einstein-deSitter universe admits a well-known parametric representation,

$$\delta(\phi) = \frac{9}{2} \frac{(\phi - \sin \phi)^2}{(1 - \cos \phi)^3} - 1, \quad \delta_l(\phi) = \frac{3}{5} \left[\frac{3}{4} (\phi - \sin \phi) \right]^{2/3}$$

for $\delta_l > 0$, linear overdensity, and

$$\delta(\phi) = \frac{9}{2} \frac{(\sinh \phi - \phi)^2}{(\cosh \phi - 1)^3} - 1, \quad \delta_l(\phi) = -\frac{3}{5} \left[\frac{3}{4} (\sinh \phi - \phi) \right]^{2/3},$$

for $\delta_l < 0$, linear underdensity (see Peebles 1980),

The above solution can be also expressed directly in terms of the initial density contrast, which plays the role of the initial size of the spherical fluctuation in Eq.[28]. This way, the evolved density contrast in the perturbative regime is given by a *local-density* transformation of the linear density fluctuation,

$$\delta = f(\delta_l) = \sum_{n=1}^{\infty} \frac{\nu_n}{n!} \delta_l^n \quad (33)$$

Notice that all the dynamical information in the SC model is encoded in the ν_n coefficients of this local-density transformation (see Eq.[33]).

In an Einstein-de Sitter universe (spatially flat universe), we can introduce the latter power series expansion in Eq.[28] and determine the ν_n coefficients one by one. The first ones turn out to be,

$$\begin{aligned} \nu_2 &= \frac{34}{21} \sim 1.62 \\ \nu_3 &= \frac{682}{189} \sim 3.61 \\ \nu_4 &= \frac{446440}{43659} \sim 10.22 \\ \nu_5 &= \frac{8546480}{243243} \sim 35.13 \end{aligned} \quad (34)$$

and so on.

Remember that this evolution is in *Lagrangian* space, $\delta = \delta(\mathbf{q})$. We would like to relate the above results, obtained in Lagrangian coordinates to the corresponding fluctuation in Eulerian coordinates. In Lagrangian space a fluid element of a given mass is labeled by its initial position \mathbf{q} (or Lagrangian coordinate), whereas Eulerian space uses the density $\rho(x)$ at the final coordinate $\mathbf{x} = \mathbf{x}(\mathbf{q})$. Notice that mass conservation requires that the volume elements be related like: $d^3 \mathbf{q} = (1 + \delta) d^3 \mathbf{x}$. Thus density probabilities in Lagrangian (_L) and Eulerian (_E) space should also be related by the same factor, $\Delta_L \delta = (1 + \delta) \Delta_E \delta$ (see Kofman et al. 1994). This provides a simple way to translate density moments in Eulerian space, $\langle (1 + \delta)^J \rangle_E$ with the ones in Lagrangian space $\langle (1 + \delta)^J \rangle_L$. We have:

$$\begin{aligned} \langle (1 + \delta)^J \rangle_L &= \int (1 + \delta)^J P[\delta] \Delta_L \delta = \\ \int (1 + \delta)^{J+1} P[\delta] \Delta_E \delta &= \langle (1 + \delta)^{J+1} \rangle_E. \end{aligned} \quad (35)$$

In particular, as pointed out by Bernardeau (B94b) (and also PS97), the conservation of Eulerian volume means:

$$\langle 1 \rangle_E = 1 = \langle (1 + \delta)^{-1} \rangle_L \quad (36)$$

which requires a normalization for δ in Eq.[33]:

$$1 + \delta = (1 + f) \langle (1 + f)^{-1} \rangle_L. \quad (37)$$

It is interesting to note from Eq.[35] that:

$$\langle \delta^J \rangle_L = \langle \delta^J \rangle_E + \langle \delta^{J+1} \rangle_E, \quad (38)$$

Thus, to leading order, there is no difference between Eulerian or Lagrangian moments. In general, the leading contribution to the cumulants is enough to specify all the coefficients c_n , e.g. Eq.[21], of the local transformation provided

by Eq.[19]. This means that the local-density transformations that produce the tree-level in PT are identical in Euler and Lagrangian space. A similar result was noted by Protopingers & Scherrer (PS97), in the context of hierarchical distributions, but this argument is more general and it applies to any non-Gaussian distributions were: $\langle \delta^{J+1} \rangle_E < \langle \delta^J \rangle_E$, which holds even for the strongly non-Gaussian dimensional models Eq.[8] that we shall investigate later (see Paper II).

3.2 The SC as a solution for the cumulants

Our goal is to relate the cumulants in the initial distribution with the ones resulting from the full non-linear evolution of the field. To estimate the evolved cumulants under the spherical collapse dynamics, we perform the following prescription:

- (a) we start with the initial cumulants, in the limit of small fluctuations, $\delta \rightarrow 0$. In this limit, the cumulants are equal in Lagrangian and Eulerian space, as $d^3 \mathbf{q} \rightarrow d^3 \mathbf{x}$.
- (b) we next use the local transformation Eq.[33], with its proper normalization Eq.[37], to relate the initial and final cumulants in Lagrangian space. As argued above this is equivalent to include the contribution from the monopole alone. This can be done as described in section §2.6 using Eq.[20] to obtain expressions such as Eq.[21] by keeping the relevant terms.
- (c) finally we use Eq.[35] to relate the Lagrangian and Eulerian moments, which can be rewritten, in a more compact way:

$$\langle \delta^J \rangle_E = \langle \delta^{J-1} \rangle_L - \langle \delta^{J-2} \rangle_L + \langle \delta^{J-3} \rangle_L - \dots + \langle \delta \rangle_L, \quad (39)$$

from which we get the cumulants.

Note that the cumulants obtained from (b)+(c), which are given by Eq.[A2], are not the same as the ones obtained using the local-density relation in *Euler* space directly, e.g. §B. As explicitly seen from Eq.[38], they are only the same to leading order. We choose this approach because the Lagrangian space, comoving with the fluid element, is the natural coordinate system for a local description of its evolution. Note that a local-density description in Lagrangian space will in general mean a non-local one in Euler space.

3.3 The SC model and Perturbation Theory

We have pointed out in the previous sections that the monopole contribution (which is the exact result for tree-graphs) to the cumulants in PT is given by a local-density transformation Eq.[19], whose coefficients c_n are to be determined by the kernels F_n (see Eq.[4]) under the relevant dynamics. These arguments are valid for any dynamics and apply either to Euler or Lagrangian space, they are true for any leading order calculation. As argued in section §(2.7), to estimate this contribution to the cumulants it is not necessary to calculate the full kernels F_n , as we only need the numbers c_n . Given the equations for the evolution of a field, one can determine Eq.[19] and therefore c_n by just requiring the solutions to be *spherically symmetric*.

We have shown above that for gravity, the spherically symmetric solution to the dynamical equations is given by Eq.[27], e.g. the SC, whose solution is well-known (see

Eq.[33]). Thus, $\mathcal{L} = f$ which the monopole contribution, $c_n = \nu_n$, without need of estimating the kernels F_n or any integral. Note, in particular, how $\nu_2 = 34/21$ (see Eqs.[16],[34]).

This provides with a simpler derivation and interpretation for the results presented by B92, who found the values ν_n that give the leading order contribution to PT for GIC. In the language of B92, the vertex generating function, $\mathcal{G}(-\tau) = \{(\delta_\dagger)\}$ (see also PS97). Our derivation explains therefore why the vertex generating function $\mathcal{G}(-\tau)$ follows the SC model, which lacked a satisfactory explanation in the context of B92. Besides its simplicity, in our framework one has the added advantage of being able to use the local-density relation to estimate the higher-order corrections for both GIC and NGIC (see Paper II). Note nevertheless that there is an important difference in practice with the work of B92. His vertex generating function $\mathcal{G}(-\tau)$, corresponds to cumulants in Euler space, while our local-density relation $f(\delta_\dagger)$, applies to Lagrangian space. To leading order, both give identical results for GIC, but they yield different results in general for Non-Gaussian IC or for next-to-leading-terms for GIC.

We want to stress that the fact the SC model determines the tree-level amplitudes is neither a singular property of the Gaussian nature of the IC nor an argument that has to do with the flat geometry of space, but something rather general which follows straightforwardly from the *local* nature of the monopole contribution to PT (see section §2.7): *the tree-graphs (and the monopole contribution) in PT are exactly given by the SC model regardless of either the statistical nature of the initial conditions or the geometry of the universe*. We shall illustrate the above statement in the framework of B92 calculations by showing, in a forthcoming paper (Paper III), that the equations of motion that govern the leading order amplitudes for GIC in a universe with arbitrary density parameter Ω , are nothing but those of the SC dynamics.

3.4 Smoothing effects

So far we have worked out the statistics of the unsmoothed fields. There remains to be seen whether the local-density approximation may be extended to the statistics of the spatially smoothed fields, which is essential if we are to compare with N-body simulations and observations. Our goal is therefore to relate the *smoothed* cumulants in the evolved distribution with the *smoothed* cumulants in the initial one. The latter are *inputs* to our calculations, e.g. how the smoothed rms fluctuation changes as a function of the smoothing radius: $\hat{\sigma} = \hat{\sigma}(R)$.

We will focus here in the top-hat filter,

$$W_{TH}(\mathbf{x}, R) = 1 \quad \text{if} \quad \mathbf{x} \leq R,$$

being zero otherwise, where R is the smoothing radius. Note that this filter is spherically symmetric so that the transformation that gets from the unsmoothed to the smoothed evolved fields preserves the spherical symmetry.

In the local-density picture of the spherical collapse, each fluctuation is isolated from the others and evolves according to the value of the initial amplitude alone. The statistics of the evolved field are just induced by the statistics of the initial one, which could in general be non-Gaussian. In order to estimate the statistical properties

(one-point cumulants) we can therefore picture the initial spatial distribution as just made of a single spherical fluctuation. Different realizations of this fluctuation could have different amplitudes or shapes in a proportion given so as to match the statistics of the initial conditions (see §61 Peebles 1980 for examples). In our case this is given in terms of the *un-smoothed* distribution, which corresponds to a top-hat smoothing of radius $R_0 \rightarrow 0$.

The spatial smoothing only acts on the fluctuation by changing its amplitude. We want, by construction, the new amplitude to be a function of the smoothing radius, R . Thus, for the initial conditions δ_l , the smoothed field is:

$$\hat{\delta}_l(R) = \frac{\hat{\sigma}_l(R)}{\sigma_l(R_0)} \delta_l \quad (40)$$

as smoothing does not change the statistics directly. A similar argument applies to the evolved field, which under the SC model is just a local transformation of the initial fluctuations, which only changes the local amplitude:

$$\hat{\delta} = \frac{\hat{\sigma}}{\sigma} \delta \quad (41)$$

where $\hat{\delta}$ is the smoothed fluctuation and δ the unsmoothed one. The statistics of $\hat{\delta}$ will therefore be given by the unsmoothed statistic, δ , which are, in its turn, given by the local-density relation Eq.[33]:

$$\hat{\delta} \sim \delta = f[\delta_l]. \quad (42)$$

Using Eq.[40] we express this as a function of the linear smoothed fluctuation $\hat{\delta}_l$:

$$\hat{\delta}[\hat{\delta}_l] \sim f[\hat{\delta}_l \frac{\sigma_l}{\hat{\sigma}_l}] \quad (43)$$

where \sim just means that $\hat{\delta}$ needs to be normalized, as explained before (see Eq.[37]). Note that the input rms is a function of the smoothing radius, R , which also sets the amplitude of the final smoothed fluctuation. Mass conservation requires: $d^3\mathbf{q} = (1 + \delta)d^3\mathbf{x}$, which for the smoothed fluctuation means:

$$1 + \hat{\delta} \sim R^{-3} \quad (44)$$

Thus the smoothed amplitude $\hat{\sigma} = \hat{\sigma}[R]$ will be a function of $\hat{\delta}$ through R . This together with Eq.[43] can be used to obtain $\hat{\delta}$ in a recursive way.

In the case of a power-law power spectrum $P(k) \sim k^n$, the smoothed variance is also a power-law $\hat{\sigma}_l \sim R^{\gamma/2}$, were $\gamma = -(n + 3)$. We then have:

$$\hat{\sigma}_l = \sigma_l (1 + \hat{\delta})^{-\gamma/6}. \quad (45)$$

Note that $\gamma = 0$ reproduces the unsmoothed result. So that using Eq.[43], we find:

$$\hat{\delta}[\hat{\delta}_l] \sim f[\hat{\delta}_l (1 + \hat{\delta})^{\gamma/6}] \quad (46)$$

up to a normalization factor given by Eq.[37]. Note that this final result as well as the general expression Eq.[43], agrees with B94a arguments, based on the vertex generating function, but they do not limit to GIC or the leading order term. Here again, the vertex generating function $\mathcal{G}(-\tau)$, corresponds to cumulants in Euler space, while our local-density relation $f(\delta_l)$, applies to Lagrangian space. To leading order, they both give identical results with GIC, but

they yield different results in general for NGIC or for higher order terms with GIC.

We will further write the smoothed density contrast (over a smoothing scale R) in the following way:

$$\hat{\delta} = \hat{f}(\hat{\delta}_l) \equiv \sum_{k=1}^{\infty} \frac{\bar{\nu}_k}{k!} (\hat{\delta}_l)^k, \quad (47)$$

where the $\bar{\nu}_k$ are a generalization of the unsmoothed coefficients. By Taylor-expanding Eq.[46] one obtains,

$$\begin{aligned} \bar{\nu}_2 &= \nu_2 + \frac{\gamma}{3} \\ \bar{\nu}_3 &= \frac{1}{4}(-2\gamma + \gamma^2 + 6\gamma\nu_2 + 4\nu_3) \\ \bar{\nu}_4 &= \frac{1}{27}(36\gamma - 36\gamma^2 + 8\gamma^3 - 108\gamma\nu_2 + 72\gamma^2\nu_2 + \\ &+ 54\gamma\nu_2^2 + 72\gamma\nu_3 + 27\nu_4). \end{aligned} \quad (48)$$

For an arbitrary power-law $P(k)$, the above results trivially generalize using Eq.[43] and they are given in Eq.[A4] of the Appendix §A3.

In Appendix §C we present an alternative derivation for the (top-hat) smoothing effects within the spherical collapse, following the kernels in Fourier space. There, one can see explicitly how in the SC model, smoothing is a trivial operation which only changes the ν_n coefficients but not the local nature of the transformation.

4 COMPARISON OF THE SC MODEL WITH EXACT PT AND N-BODY SIMULATIONS

In this section we start from the exact solution to the SC dynamics in an Einstein-de Sitter universe assuming the rms density fluctuation $\sigma_l \lesssim 1$. In that perturbative limit, we carry out the calculation of the connected moments for the density. Results for the velocity field are provided in Paper III.

We compare the SC predictions with those derived from the exact PT in the context of the diagrammatic approach. Although we know that the SC dynamics reproduces exactly the leading order contribution to the cumulants, higher order effects will in general be different. We have seen that the difference is due to neglecting the shear and can therefore be attributed to non-local effects, which we will also call *tidal* effects. Note that in our context *local* refers only to the density.

As commented above, the results are derived in general for the smoothed fields for a top-hat window function, the unsmoothed fields being recovered just as the particular case $\gamma = 0$. To simplify the expressions, we will assume that higher order derivatives of the variance Eq.[A4] can be neglected, $\gamma_p \simeq 0$ for $p > 2$. This is a good approximation for slowly varying $P(k)$, like CDM (see Scoccimarro 1998) or the APM model, but it is straight forward to take them into account anyway. We do take into account γ_2 , which for loop corrections could contribute up to 10% at small scales.

We will also compare the SC results with different N-body simulations, with parameters given in Table 1. Also given is the reference where the details for a particular run can be found. For each simulation, the cumulants $\bar{\xi}_J$ are estimated from counts in spherical cells, as described in BGE95, where more details about the estimation are given. For the

later outputs the correlations are corrected from the Poisson shot-noise (e.g. BGE95). We also apply the corrections due to the ZA transient (see Baugh et al 1995) as derived by Scoccimarro (1998).

Following the steps described in section §3.2, we can derive now the smoothed one-point cumulants to an arbitrary perturbative order for the SC dynamics. In this case we start from GIC and use the local transformation for the local smoothed density (see Eq.[47]) with $c_k = \bar{\nu}_k$ as given in Eq.[48], to find the leading order and higher order corrections for the variance and the hierarchical amplitudes. To handle the perturbative expansions in the cumulants for both GIC or NGIC in a general framework, we shall introduce the following notation

$$\sigma^2 = \langle \hat{\delta}^2 \rangle = \sum_i s_{2,i} \sigma_l^i \quad (49)$$

where $s_{2,1} \equiv 1$ and the subscript in the coefficients label the order of the perturbative expansion. For GIC the odd terms in the perturbative expansion vanish and the latter expression boils down to,

$$\sigma^2 \equiv \sigma_G^2 = \sigma_l^2 + s_{2,4} \sigma_l^4 + s_{2,6} \sigma_l^6 + \dots \quad (50)$$

Note that our notation for GIC is equivalent to that of SF97a provided one identifies $s_{2,2i+2} \equiv s^{(i)}$ with $i = 1, 2, \dots$.

On the other hand, for the hierarchical amplitudes we keep the above introduced notation with the added labeling of the order of the moment J , that defines the S_J coefficients,

$$S_J \equiv \frac{\xi_J}{\xi_2^{J-1}} \equiv \frac{\langle \hat{\delta}^J \rangle_c}{\langle \hat{\delta}^2 \rangle^{J-1}} = \sum_i S_{J,i} \sigma_l^i \quad (51)$$

which for GIC has non-vanishing contributions from the even terms alone,

$$S_J^G = S_{J,0} + S_{J,2} \sigma_l^2 + S_{J,4} \sigma_l^4 + \dots \quad (52)$$

where $S_{J,2i} \equiv S_J^{(i)}$ (with $i = 0, 1, 2, \dots$) in SF97a notation.

As mentioned before, it is usual to denote *tree-level* to the leading order contributions, $S_J^{(0)}$. Although this is true for GIC, in general the leading order contributions do not correspond to the tree-level in the diagrammatic approach (see Paper II). However, for the sake of clarity, we shall maintain the notation $S_J^{(0)}$ (or $T_J^{(0)}$ for the velocity fields, see Paper III) to denote the leading-order contribution.

With this notation the results for GIC in terms of the SC coefficients ν_k are given in Eq.[A2] with $c_k = \nu_k$. In terms of the smoothing index γ we have:

$$\begin{aligned} s_{2,4} &= \frac{1909}{1323} + \frac{143}{126} \gamma + \frac{11}{36} \gamma^2 \\ s_{2,6} &= \frac{344439415}{107270163} + \frac{21651395}{3667356} \gamma + \frac{408721}{95256} \gamma^2 + \\ &+ \frac{1651}{1134} \gamma^3 + \frac{127}{648} \gamma^4 \\ S_{3,0} &\equiv S_3^{(0)} = \frac{34}{7} + \gamma \\ S_{3,2} &= \frac{1026488}{101871} + \frac{12862}{1323} \gamma + \frac{407}{126} \gamma^2 + \frac{10}{27} \gamma^3 \\ S_{3,4} &= \frac{251978977148}{5256237987} + \frac{71492200235}{750891141} \gamma + \frac{138567091}{1833678} \gamma^2 \\ &+ \frac{79295}{2646} \gamma^3 + \frac{2891}{486} \gamma^4 + \frac{1841}{3888} \gamma^5 \end{aligned}$$

SC	Unsmoothed				Smoothed			
	$\gamma = 0$	$\gamma = -1$	$\gamma = -2$	$\gamma = -3$	$n = -3$	$n = -2$	$n = -1$	$n = 0$
$s_{2,4}$	1.44	0.61	0.40	0.79				
$s_{2,6}$	3.21	0.34	0.05	0.68				
$S_{3,0}$	4.86	3.86	2.86	1.86				
$S_{3,2}$	10.08	3.21	0.59	-0.02				
$S_{3,4}$	47.94	3.80	0.07	0.06				
$S_{4,0}$	45.89	27.56	13.89	4.89				
$S_{4,2}$	267.72	63.56	7.39	-0.16				
$S_{4,4}$	2037.2	138.43	1.99	0.31				
$S_{5,0}$	656.31	292.35	96.50	16.52				
$S_{5,2}$	7242.2	1263.97	91.85	-1.16				
$S_{5,4}$	80903.0	4363.92	42.89	1.53				
$S_{6,0}$	12653.49	4141.58	876.62	67.81				
$S_{6,2}$	221597.1	28256.19	1274.38	-8.04				
$S_{6,4}$	3405857.8	140641.3	906.74	7.88				

Table 2. Values for the higher-order perturbative contributions in the SC dynamics for the unsmoothed ($n = -3$) and smoothed ($n = -2, -1$) density fields.

$$\begin{aligned} S_{4,0} &\equiv S_4^{(0)} = \frac{60712}{1323} + \frac{62}{3} \gamma + \frac{7}{3} \gamma^2 \\ S_{4,2} &= \frac{22336534498}{83432349} + \frac{42649448}{130977} \gamma + \frac{3571621}{23814} \gamma^2 \\ &+ \frac{35047}{1134} \gamma^3 + \frac{1549}{648} \gamma^4 \\ S_{4,4} &= \frac{126152927186426522}{61923739724847} + \frac{69638296109567}{15768713961} \gamma \\ &+ \frac{8977285860007}{2252673423} \gamma^2 + \frac{7018518515}{3667356} \gamma^3 \\ &+ \frac{24548155}{47628} \gamma^4 + \frac{668971}{9072} \gamma^5 + \frac{102005}{23328} \gamma^6 \\ S_{5,0} &\equiv S_5^{(0)} = \frac{200575880}{305613} + \frac{1847200}{3969} \gamma + \frac{6940}{63} \gamma^2 + \frac{235}{27} \gamma^3 \\ S_{5,2} &= \frac{38066642685488}{5256237987} + \frac{8041429493780}{750891141} \gamma + \frac{5828197535}{916839} \gamma^2 \\ &+ \frac{45012655}{23814} \gamma^3 + \frac{955895}{3402} \gamma^4 + \frac{4052}{243} \gamma^5 \\ S_{6,0} &\equiv S_6^{(0)} = \frac{351903409720}{27810783} + \frac{3769596070}{305613} \gamma + \frac{17907475}{3969} \gamma^2 \\ &+ \frac{138730}{189} \gamma^3 + \frac{1210}{27} \gamma^4 \\ S_{6,2} &= \frac{93347762463213320}{421249930101} + \frac{2034255356621746}{5256237987} \gamma \\ &+ \frac{211757079765188}{750891141} \gamma^2 + \frac{301575001360}{2750517} \gamma^3 \\ &+ \frac{69888305}{2916} \gamma^4 + \frac{1582214}{567} \gamma^5 + \frac{14591}{108} \gamma^6 \end{aligned} \quad (53)$$

In table 2 we display a summary of results for the SC

Table 1. Simulation parameters

run names	$P(k)$	$\Omega-\Lambda$	number of particles	mesh	L_{box} (h^{-1} Mpc)	Reference
SCDM (a)-(j)	$\Gamma = 0.5$ CDM	$\Omega = 1 \ \Lambda = 0$	126 ³	128 ³	378	Gaztañaga & Baugh 1995
LCDM (a)-(j)	$\Gamma = 0.2$ CDM	$\Omega = 0.2 \ \Lambda = 0.8$	126 ³	128 ³	378	Gaztañaga & Baugh 1995
APMPK1 (a)-(e)	APM	$\Omega = 1 \ \Lambda = 0$	126 ³	128 ³	400	Gaztañaga & Baugh 1997
APMPK2 (a)-(b)	APM	$\Omega = 1 \ \Lambda = 0$	200 ³	128 ³	600	Baugh & Gaztañaga 1996

dynamics for different values of the spectral index. Note, to start with, that for large n or more negative γ the coefficients decrease with the order, indicating some type of convergence. For $\gamma = 0$ or $n = -3$ the coefficients of each order in the expansion increases quickly with the order, which might indicate that the PT expansion does not converge, at least in this approximation.

For S_J , there is a suppression of non-linearities with the effects of smoothing (as n increases from -3 to 0), which is also found in perturbation theory (ref?). In particular, vanishing non-linearities are found for $n \approx 0$.

4.1 Comparison with exact PT

The tree-level results are of course identical to the ones estimated by Juskiewicz et al. 1993, and B94b. For the *unsmoothed* fields, analytic results including the first corrective term to the tree-level, were first derived by SF97a through loop calculations in the diagrammatic approach to the exact PT. For the variance, skewness, and the kurtosis (the latter only at tree-level) they obtain,

$$\begin{aligned} \sigma^2 &\approx \sigma_l^2 + 1.82 \sigma_l^4 + \mathcal{O}(\sigma_{\ddagger}^{\gamma}) \\ S_3 &\approx 4.86 + 9.80 \sigma_l^2 + \mathcal{O}(\sigma_{\ddagger}^{\Delta}) \\ S_4 &\approx 45.89 + \mathcal{O}(\sigma_{\ddagger}^{\epsilon}), \end{aligned} \quad (54)$$

as the average values in the range $2 \geq n \geq -2$, with a 3% variation within that range due to non-local effects. The latter results are to be compared to those from the SC in the perturbative regime (truncated at the same order),

$$\begin{aligned} \sigma^2 &\approx \sigma_l^2 + 1.44 \sigma_l^4 + \mathcal{O}(\sigma_{\ddagger}^{\gamma}) \\ S_3 &\approx 4.86 + 10.08 \sigma_l^2 + \mathcal{O}(\sigma_{\ddagger}^{\Delta}) \\ S_4 &\approx 45.89 + 267.72 \sigma_l^2 + \mathcal{O}(\sigma_{\ddagger}^{\epsilon}). \end{aligned} \quad (55)$$

Comparing with the exact PT result (54), we can see that tidal (non-local) effects only amount to a 3% in the corrective term for S_3 and up to 20% in the first corrective term for the variance. The S_4 correction ($\sim 268 \sigma_l^2$) must be taken as an accurate prediction for S_4 (within the few per cent effect coming from the tidal forces) since there are no analytic results available to compare with. We therefore see from the above comparison that the shearless (SC) approximation leads to very accurate predictions for the hierarchical

amplitudes, S_J , while giving worse estimates for the cumulants ξ_J .

For the *smoothed* fields, there are few analytic results which concentrate on the variance (and power-spectrum), the skewness, and the bispectrum. For the present analysis we focus on the results for the variance and the skewness (see SF97b and Scoccimarro 1997, hereafter S97, respectively) which in the diagrammatic approach to the exact PT to one-loop order for a top-hat smoothing and $n = -2$, give

$$\begin{aligned} \sigma^2 &\approx \sigma_l^2 + 0.88 \sigma_l^4 + \mathcal{O}(\sigma_{\ddagger}^{\gamma}) \\ S_3 &\approx 3.86 + 3.18 \sigma_l^2 + \mathcal{O}(\sigma_{\ddagger}^{\Delta}) \end{aligned} \quad (56)$$

that we compare to the SC predictions,

$$\begin{aligned} \sigma^2 &\approx \sigma_l^2 + 0.61 \sigma_l^4 + \mathcal{O}(\sigma_{\ddagger}^{\gamma}) \\ S_3 &\approx 3.86 + 3.21 \sigma_l^2 + \mathcal{O}(\sigma_{\ddagger}^{\Delta}) \end{aligned} \quad (57)$$

which means a 30% and 1% contribution from the tidal forces for the corrections in the variance and the skewness respectively (these can be obtained by just subtracting the shearless (SC) contribution to the exact computation carried by means of the loop calculations). Thus, we see that in line with the unsmoothed predictions, the shearless contribution completely dominates the skewness S_3 , at least at the one loop order.

In Fig 1 we display the departures from the tree-level contribution for the evolved variance, skewness and kurtosis as the linear variance approaches unity where the perturbative regime is expected to break down. Fig 2 shows the same as Fig 1 when the 3rd. perturbative order (second corrective term) is included in the computation of the cumulants: the qualitative features are preserved when this higher-order contribution is taken into account with respect to those inferred from the 2nd. order analysis, with a monotonous enhancement of the scaling properties.

In Table 2 we compare the results from different approximations to the exact dynamics in the perturbative regime (exact PT), available in the literature and we give as well the SC predictions in the same regime. We recall that the FFA is based on a linearization of the peculiar velocity field. The LPA assumes the potential remains linear throughout the gravitational evolution, and the ZA takes the trajectories of the particles to be straight lines. All values concerning the 1-loop contribution (including the exact PT ones), except for the SC ones, are derived making use of the diagram-

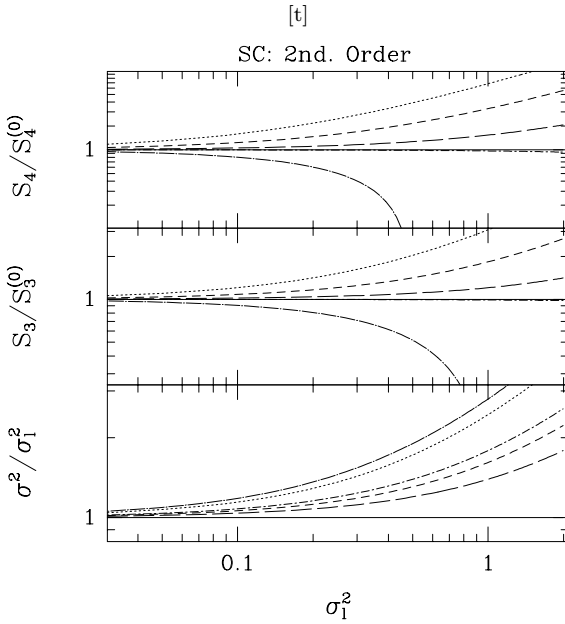


Figure 1. Departures from the tree-level contributions as the linear rms fluctuation grows, for the variance, skewness and kurtosis of the density field as predicted by the SC model up to the 2nd. non-vanishing perturbative order (first corrective term) for different values of the spectral index: the dotted line shows the $n = -3$ (unsmoothed) case, and the short-dashed ($n = -2$), long-dashed ($n = -1$), dot short-dashed ($n = 0$), dot long-dashed ($n = 1$) depict the behaviour for the smoothed density field. The solid line shows the tree-level values as a reference. The corrective term has a minimum contribution to the variance for $n \approx -1$, while the hierarchical amplitudes show a vanishing second order contribution for $n \approx 0$.

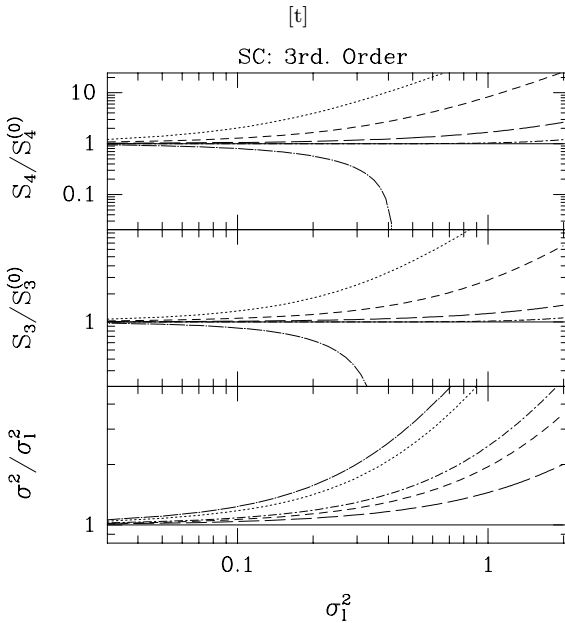


Figure 2. Same as Fig 1 when the 3rd. perturbative order is included in the computation of the cumulants.

Dynamics	$s_{2,4}$	$S_{3,0}$	$S_{3,2}$	$S_{4,0}$	$S_{4,2}$
<i>FFA*</i>	0.43	3	1	16	15.0
<i>LPA*</i>	0.72	3.40	2.12	21.22	37.12
<i>ZA*</i>	1.27	4	4.69	30.22	98.51
<i>SC</i>	1.44	4.86	10.08	45.89	267.72
<i>Exact PT*</i>	1.82	4.86	9.80	45.89	?

Table 3. Comparison between different non-linear approximations to the for the *unsmoothed* fields up to the first corrective term beyond tree-level. The asterisk denotes the results obtained within the diagrammatic approach for the relevant dynamics.

matical formalism and are given in SF97a. Tree-level amplitudes had been derived previously though and a summary of those results may be found in Bernardeau et al. 1994.

As can be seen in the Table 3, the SC model is by far the closest to the exact PT results.

4.2 Previrialization in the variance

It is important to notice the different behaviour between the cumulants (like the variance) and the hierarchical amplitudes S_J . It has long been argued that non-local effects generate a suppression of collapse on the largest scales due to the increase in small-scale power that generates large scale random motions, the so-called effect of *previrialization* (see Davis and Peebles 1977, Peebles 1990, Lokas et al. 1996). This will result in a non-linear variance that is smaller than the linear one within a certain range. This effect has been found in N-body simulations (e.g. see Figure 9 in BGE95).

The local picture arising from the SC dynamics is unable to account for a complete suppression of non-linearities in the large scale density (and velocity) fields and yields a faster growth of fluctuations on the large scales compared to the actual non-local dynamics. This suppression depends on the smoothing effects and leads to the appearance of a critical value of the spectral index (assuming scale free power spectrum) around $n_c \approx -1.4$ (see S97), for which non-linear contributions vanish. Figs 1 and 2 illustrate well this point since no change of sign in the first non-linear contribution (beyond tree-level) to the evolved variance is appreciated in the plot contrary to what has been found in numerical simulations depicting the exact perturbative scaling (see Lokas et al. 1996, Fig 4). Note that the SC prediction yields a minimum contribution at $n \simeq -1.14$, which is not far from $n_c \approx -1.4$, but the net effect at the minimum is non-zero.

Comparing the results for the variance from the exact PT and the shearless (SC) approximation, we can infer some information about where the tidal effects become lower, comparable or greater than the shearless contribution, provided the variance changes smoothly. Let us formally decompose the one-loop contribution to the variance in the shearless and tidal contributions as follows,

$$s_{2,4} = s_{2,4}^{SC} + s_{2,4}^{Tide} \quad (58)$$

where $s_{2,4}^{SC} > 0$ for all n as displayed on the bottom panel of Fig 1. According to the above results, there is a critical value

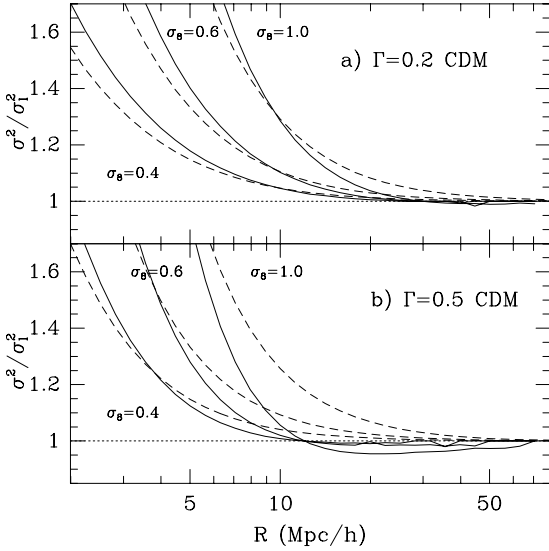


Figure 3. The variance in spherical shells of radius R . We compare linear theory with the SC model and the exact PT (leading order) non-linear correction. Each panels, (a) and (b), show the ratio of the non-linear to the linear variance for the $\Gamma = 0.2$ (a) or $\Gamma = 0.5$ (b) CDM initial $P(k)$. In both cases the continuous line from bottom to top corresponds to $\sigma_8 = 0.4, 0.6, 1.0$. The SC predictions for the same amplitudes are shown as dashed lines.

$n_c \simeq -1.45$ where the total contribution vanishes $s_{2,4} = 0$, so that $s_{2,4}^{SC} = -s_{2,4}^{Tide}$, and at $n = -2$ we have from (57) that $s_{2,4} > s_{2,4}^{SC} > 0$. This means that $s_{2,4}^{Tide}$ changes sign: first ($n=-3$) the tidal contribution takes positive values and decreases as n increases up to some value $n_* \in [-1.45, -2]$ at which tidal effects vanish and thus, $s_{2,4} = s_{2,4}^{SC}$. Therefore, in this range, the SC model must lead to accurate estimates of the exact computation of the variance.

On the other hand, for $n > n_c$ tidal effects take over the non-linear terms as is immediately implied by the fact that $s_{2,4}$ progressively takes larger negative values as seen in numerical simulations (see Lokas et al. 1996), contrary to what the SC model predicts, so that, in that range: $|s_{2,4}^{Tide}| > |s_{2,4}^{SC}|$, which roughly represents the point beyond which the shearless approximation breaks down as far as the variance is concerned.

In Figure 3 we compare the non-linear evolution of the variance for SC and PT. We present the ratio of the non-linear to the linear variance from CDM model, with $\Gamma = 0.2$ (top panel) and $\Gamma = 0.5$ (bottom), as a function of the smoothing radius. The leading order non-linear SC predictions are shown as dashed lines. The corresponding (numerically integrated) PT results are shown as continuous lines. These are estimated from $P(k)$ in second order PT as obtained following Baugh & Efstathiou (1994). In both cases we show results for different amplitudes of the linear variance: $\sigma_8 = 0.4, 0.6, 1.0$, which has a linear variance $\sigma \simeq 0.5$ at scales $R \simeq 6, 10, 15 h^{-1}$ Mpc, respectively. We can define an *effective index*, n_{eff} , as the index at the scale where the variance becomes unity. For $\Gamma = 0.2$ model we have that $n_{eff}^{\Gamma=0.2} \simeq -2$, while for $\Gamma = 0.5$ this is about 0.5 larger (this can be seen for example in Figure 9 in Croft & Gaztañaga

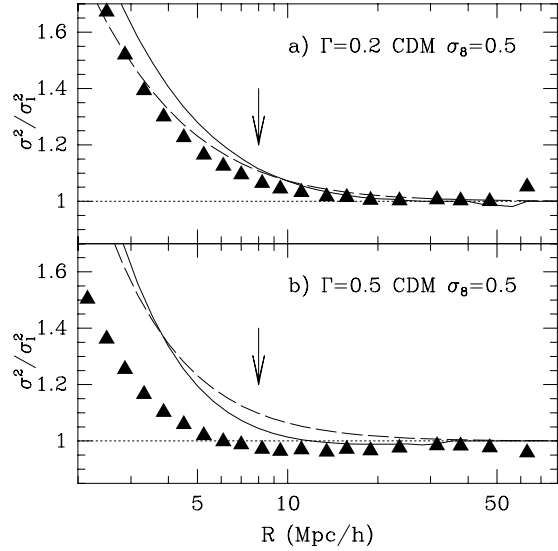


Figure 4. Non-linear evolution of the variance. Symbols show the ratio of the non-linear to the linear variance from CDM N-body simulations with $\Gamma = 0.2$ (top panel) and $\Gamma = 0.5$ (bottom panel) as a function of the smoothing radius. In both cases $\sigma_8 = 0.5$. The SC model predictions are shown as a short-dashed line while PT theory predictions are shown as a continuous line. The arrows indicate where $\sigma_l = 0.5$.

1997b): $n_{eff}^{\Gamma=0.5} \simeq -1.5$. The SC prediction should match better the $\Gamma = 0.2$ model, as the effective index is closer to n_* , where tidal effects vanish. For the $\Gamma = 0.5$ model we have that $n_{eff} \simeq n_c$ and the SC model is not such a good approximation. In this case we expect non-linear effects to be small due to the cancellation of tidal and purely local forces. This can be seen in Figure 3. The SC model matches well the PT prediction for the $\Gamma = 0.2$ model, where non-linear effects are more important. It also matches well the initial evolution of $\Gamma = 0.5$ model, for small amplitudes of σ_l , e.g. earlier outputs given by smaller σ_8 . For the later outputs, e.g. $\sigma_8 = 1$ in Figure 3 b), tidal effects become important canceling out the non-linear growth (previrialization). This is not fully recovered by the SC model (which only accounts for the local effects). Nevertheless note that for small scales, where the variance is large, the prediction seems to be dominated by the local effects and the SC model also recovers the exact prediction.

In Figure 4 we show the non-linear evolution of the variance as the ratio to the linear variance from CDM N-body simulations with $\Gamma = 0.5$ (filled triangles) and $\Gamma = 0.2$ (open triangles) as a function of the smoothing radius. The errorbars, from 10 realizations of the models, which are not displayed for clarity, are always smaller than the symbols except for the last 3 points where the errorbars are smaller than twice the size of the symbols. In both cases $\sigma_8 = 0.5$ and the linear variance $\sigma \simeq 1$ at $R \simeq 2 h^{-1}$ Mpc. The SC predictions are shown as dashed lines, which are to be compared to the exact PT results (continuous lines). For the $\Gamma = 0.2$ model there is hardly any difference between the predictions and the N-body results. In fact, the latter follows both predictions up to large values of σ (small scales).

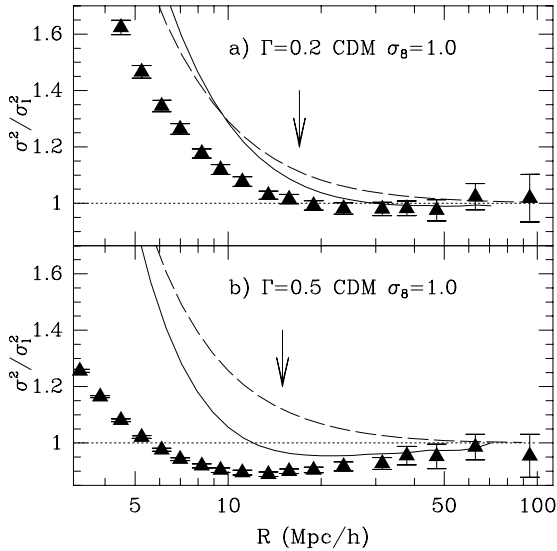


Figure 5. Same as Fig. 4 for $\sigma_8 = 1.0$.

For the $\Gamma = 0.5$ model, non-linear effects are small during the weakly non-linear phase and both linear and non-linear predictions are close to the Nbody results. There is a slight sign of previrialization at $R \simeq 20 h^{-1} \text{Mpc}$, but the effect is quite small. So although the exact PT results are more accurate in qualitative terms there is little difference in practice. Note that in this case the agreement with predictions does not extend to large values of σ (small scales) unlike the case for the $\Gamma = 0.2$ model.

Figure 5 shows the corresponding results for $\sigma_8 = 1$. In this case, the $\Gamma = 0.2$ CDM model is the one with an effective index $n_{eff} \simeq n_c$ so that non-linear effects are small and we have a similar situation to the $\Gamma = 0.5$ model at $\sigma_8 = 0.5$. The effective index for $\Gamma = 0.5$ model at $\sigma_8 = 1.0$ is $n > n_c$ so that the previrialization effect discussed above is larger and the SC prediction fails (long-dashed line). The second order PT prediction for the $\Gamma = 0.5$ is shown as a continuous line. Although it shows some previrialization effect (the ratio is smaller than unity), it only fits the Nbody results in the narrow range of scales, $R \gtrsim 30 h^{-1} \text{Mpc}$, where linear theory is a good approximation, given the errors.

The above arguments explain in a simple fashion why the SC model matches so well the variance of the APM simulations even on small scales (for output times $\sigma_8 \lesssim 1$) as shown in Fig. 6. The effective index n_{eff} on the quasi-linear scales is within the range $-2 \gtrsim n_{eff} \gtrsim -1.5$, a bit lower than the $\Gamma = 0.2$ CDM model (see Fig. 3 in BG96, where quasi-linear scales correspond to $k \simeq 0.1$). For this index, tidal effects are expected to give a subdominant contribution. Although the SC model seems to match well the simulations up to the scales where the linear variance $\sigma_l \gtrsim 1$, i.e., beyond the point where PT must break down, the third order SC correction (long-dashed line) shows deviations already at $R \simeq 6 h^{-1} \text{Mpc}$, where $\sigma_l \simeq 1$.

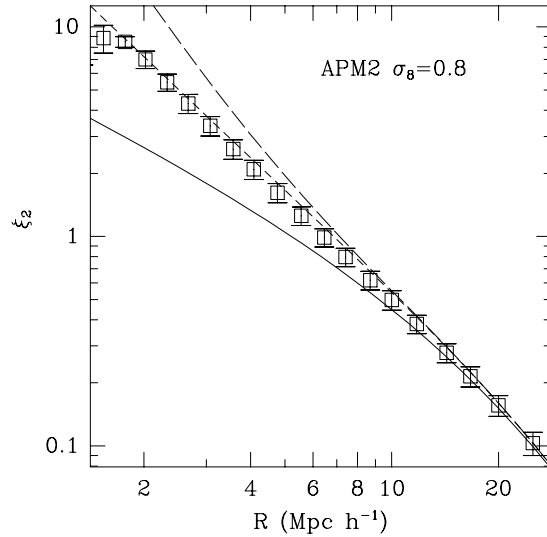


Figure 6. The variance for APMPK at $\sigma_8 = 0.8$ (figures) compared to PT models (lines): a) linear theory prediction (continuous line), b) the second order result in the SC (short dashed lines) c) the third order result in the SC (long dashed lines).

4.3 Comparison of S_J with N-body simulations: Previrialization lost

On the other hand, when it comes to evaluating the hierarchical amplitudes, S_J , it turns out that the cancellation of (non-local) tidal effects erases the previrialization effect and the suppression of non-linearities at the first corrective order beyond tree-level appears at a different spectral index $n \approx 0$, what seems to be an intrinsic (local) shearless feature if the good agreement between the local (SC) and non-local (exact PT) hierarchical amplitudes is anything to go by. Furthermore, loop-calculations in Fourier space concerning the reduced Bispectrum Q seem to confirm this argument as the scale dependence of the latter retains non-vanishing non-linearities even at $n \approx -1.5$ (at least for the equilateral configuration, see Scoccimarro et al. 1997, Eq.[30]). However, the reduced bispectrum also preserves some non-local features which manifest in terms of a loss of configuration dependence (isotropization) roughly at the same value of the spectral index as the one estimated from the variance or the power spectrum, $n_c \approx -1.4$ (see SF97b, and S97).

In Figs 7, we compare the SC predictions with CDM simulations for two different models. The smoothing coefficients $\overline{\nu_k}$ are modified to include the higher-order logarithmic derivatives of the variance (see Eq. [A3]) but it turns out that, within the errors, they do not significantly change the predictions derived from the power-law power spectrum. At small scales γ_2 changes S_3 by less than 10%, which hardly makes any difference given the errors, as shown by the dotted line, only displayed for the $\Gamma = 0.2$ $\sigma_8 = 0.05$ model for clarity. The error bars shown in the SCDM plot are derived from ten realizations. The arrows in the Figure show the scale at which $\sigma = 0.5$.

At large scales the spectral index n for CDM models becomes larger and non-linearities are very small, as pre-

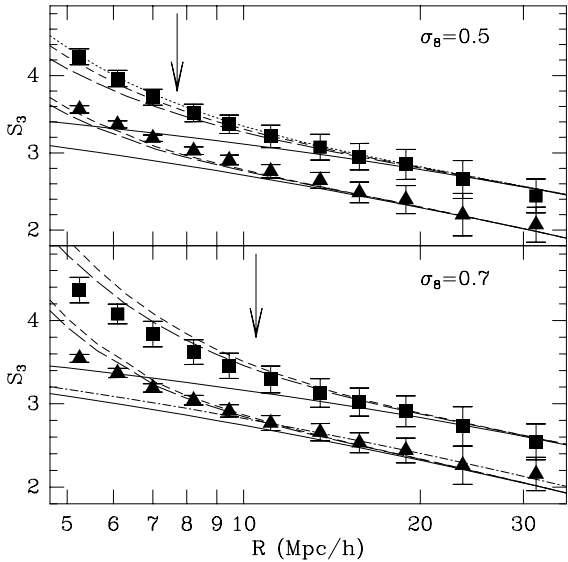


Figure 7. The hierarchical skewness S_3 from 10 realizations of flat CDM N-body simulations at output time $\sigma_8 = 0.5$ (top panel) and $\sigma_8 = 0.7$ (bottom panel). Symbols with errorbars correspond to $\Gamma = 0.2$ (squares), and $\Gamma = 0.5$ (triangles). Each case is compared to the corresponding PT predictions (lines): a) the PT tree-level prediction (continuous line), b) the second order result in the SC (short-dashed). The dotted line shows the SC prediction for the $\Gamma = 0.2$ $\sigma_8 = 0.5$ model when γ_2 is set to zero. The arrows show where $\sigma = 0.5$. The dot-dashed line shows the tree-level prediction for the $\Gamma = 0.5$ $\sigma_8 = 0.7$ uncorrected for the ZA transient.

dicted by the SC model (see Table 2). This explains why deviations from the tree-level are hardly noticeable in the later outputs (bottom panel) and they only become important when PT theory should break down ($\sigma_l \simeq 1$). The effective index in the earlier outputs is smaller (corresponding to smaller scales) and deviations from tree-level are more important. In this regime the SC predictions show a very good agreement with the Nbody (top panel) up to $\sigma \simeq 1$. Note that the predictions for the exact PT corrections are not available in this case, but the agreement with the Nbody simulations indicates that the SC models provides with an excellent approximation.

We have corrected for ZA transients, an artifact due to the initial (ZA) start in the N-body simulations (see Gazta 1995, Scoccimarro 1998). We use the results of Scoccimarro (1998) for the tree-level:

$$S_{3,0} = \frac{34}{7} + \gamma - \frac{2}{5}a^{-1} - \frac{16}{35}a^{-7/2} \quad (59)$$

where a is the expansion factor away from the (ZA) IC. In principle this is not a very important correction for the tree-level result, as the sampling errors on large scales, where σ is small, are large. This is more important for smaller scales, as the errors are smaller. In Figs 7 we show the tree-level prediction for $a \rightarrow \infty$ (dot-dashed line) as compare to the real prediction, including the transient, for $a = 5.0$ (the bottom continuous line) in the $\Gamma = 0.5$ $\sigma_8 = 0.7$ model. As pointed out by Scoccimarro, the effects of the transients tends to create the false impression that the tree-level PT has a wider

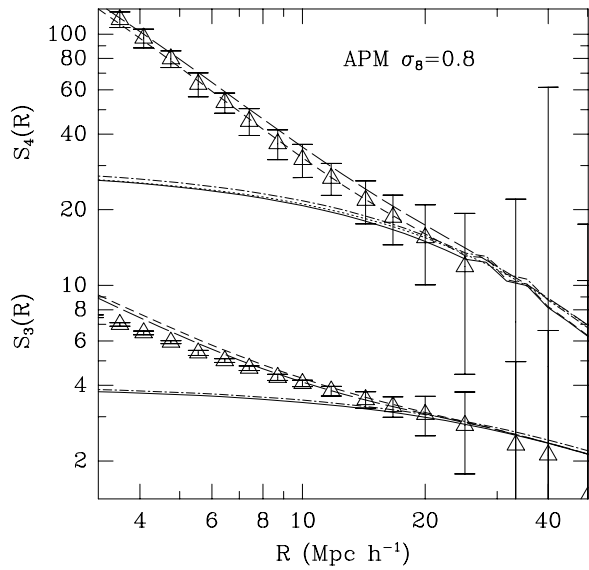


Figure 8. The skewness, S_3 , and kurtosis, S_4 for simulations of the APMPK at $\sigma_8 = 0.8$ (figures with errors) compared to tree-level theory prediction (continuous line) and the second order result in the SC (short dashed lines). The corresponding predictions for $\gamma_2 = 0$ are shown as dotted and long-dashed lines respectively. The dotted-dashed lines show the tree-level predictions uncorrected for the ZA transients.

range of validity. In our case, by comparing the points to the dotted-dashed line one might conclude that tree-level is valid up to $R \simeq 9$, while a comparison to the corrected prediction (continuous line) indicates $R \simeq 15$. On the other hand, adding the loop terms to the uncorrected tree-level would give the false impression of a poor agreement with the SC model.

Figs 8 and 9 display the scaling of the higher-order moments according to the APM-like simulations (the mean of APMPK1 and APMPK2 in Table 1). As for the previous cases, the SC model matches well the observed behaviour for the higher-orders in the N-body simulations up to the scales where PT is expected to break down, i.e., $\sigma_l \approx 1$. As we consider higher order moments, deviations from the tree-level prediction are larger, a trend that is reproduced by the SC predictions. We have found a similar trend for higher orders in the CDM models.

The ZA transients, shown as dotted-dashed lines in Fig. 8, are not very important in this case ($a \simeq 6$). The effect of using $\gamma_2 = 0$ is also small although it tends to introduce a slight shift in the predictions. For simplicity we have used $\gamma_2 = 0$ in Fig. 9, so that the agreement is slightly better than displayed.

5 BEYOND THE TREE-LEVEL IN THE ZEL'DOVICH APPROXIMATION: THE SSZA APPROXIMATION

A simple accurate description of the non-linear dynamics of the fluid elements before shell crossing (single streaming

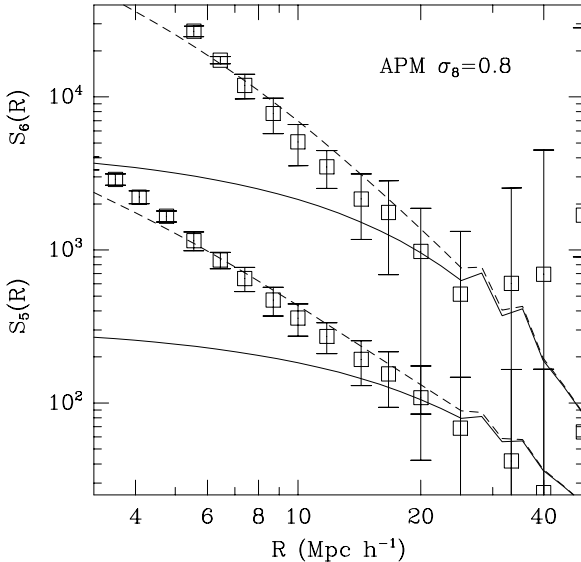


Figure 9. Same as Fig. 8 for S_5 and S_6 .

regime) is provided by the so-called Zel'dovich approximation (hereafter ZA, see Zel'dovich 1970), according to which the particle positions in comoving coordinates are assumed to follow straight lines. Despite being exact only at linear order in Lagrangian PT, the latter solution has been successfully tested as an accurate approximation, the so-called Zel'dovich Approximation (ZA) for the description of the dynamics in the non-linear regime (see also Croft & Gaztañaga 1997a). Within the ZA the fluid equations can then be easily integrated and yield,

$$1 + \delta = \prod_{i=1}^N \frac{1}{(1 - D(t) \lambda_i)} \quad (60)$$

where N is the number of spatial dimensions and $\lambda_i = -\partial \psi_i / \partial q_i$, which is in general a *non-local* relation between the displacement field and the evolved density fluctuation.

At this point we introduce the *spherically symmetric* assumption for the ZA dynamics (SSZA) as we did before with the exact dynamics and set $\lambda_i = \lambda$, i.e., all directional derivatives are equal due to the spherical symmetry (no tidal forces) and rewrite, $\delta_l = D(t) \sum_{i=1}^N \lambda_i = 3 D(t) \lambda$, where the first equality follows from the Poisson equation for the linear density contrast $\delta_l = \nabla^2 \phi_l$, with ϕ_l the initial linear gravitational potential. The latter assumption thus renders the relation (60) as a local transformation that may be expanded in power series to get the full perturbative series for the relevant statistical quantities. In particular, for the 3D case, the normalized SSZA transformation has the form,

$$\delta \sim (1 - \delta_l/3)^{-3}, \quad (61)$$

to be normalized according to (37). Notice that the latter transformation may be straightforwardly extended to any spatial dimensions. As seen in Fosalba et al. 1997, the exponential transformation that leads to the Lognormal hierarchical amplitudes, $S_J = J^{J-2}$, are only recovered when one takes the limit of infinite spatial dimensions (see also

Bernardeau and Kofman 1995), which does not make much physical sense.

Expanding (61) in power series we can determine the unsmoothed coefficients of the local non-linear transformation for the SSZA,

$$\begin{aligned} \nu_2 &= \frac{4}{3} \sim 1.33 \\ \nu_3 &= \frac{20}{9} \sim 2.22 \\ \nu_4 &= \frac{40}{9} \sim 4.44 \\ \nu_5 &= \frac{280}{27} \sim 10.37 \end{aligned} \quad (62)$$

and so forth. Introducing them in the smoothed transformation according to (48) we can now find, using equation (A3) with $c_k = \bar{v}_k$, the following results for the smoothed density field for GIC,

$$\begin{aligned} s_{2,4} &= \frac{7}{9} + \frac{11}{18} \gamma + \frac{11}{36} \gamma^2 \\ s_{2,6} &= \frac{185}{243} + \frac{535}{324} \gamma + \frac{1043}{648} \gamma^2 + \frac{127}{162} \gamma^3 + \frac{127}{648} \gamma^4 \\ S_{3,0} &\equiv S_3^{(0)} = 4 + \gamma \\ S_{3,2} &= \frac{118}{27} + \frac{16}{3} \gamma + \frac{41}{18} \gamma^2 + \frac{10}{27} \gamma^3 \\ S_{3,4} &= \frac{254}{27} + \frac{5840}{243} \gamma + \frac{12331}{486} \gamma^2 + \frac{3359}{243} \gamma^3 \\ &+ \frac{7619}{1944} \gamma^4 + \frac{1841}{3888} \gamma^5 \\ S_{4,0} &\equiv S_4^{(0)} = \frac{272}{9} + \frac{50}{3} \gamma + \frac{7}{3} \gamma^2 \\ S_{4,2} &= \frac{2506}{27} + \frac{11512}{81} \gamma + \frac{13523}{162} \gamma^2 + \frac{3679}{162} \gamma^3 + \frac{1549}{648} \gamma^4 \\ S_{4,4} &= \frac{241298}{729} + \frac{673477}{729} \gamma + \frac{791531}{729} \gamma^2 + \frac{2025815}{2916} \gamma^3 \\ &+ \frac{248275}{972} \gamma^4 + \frac{22141}{432} \gamma^5 + \frac{102005}{23328} \gamma^6 \\ S_{5,0} &\equiv S_5^{(0)} = \frac{3080}{9} + \frac{8060}{27} \gamma + \frac{790}{9} \gamma^2 + \frac{235}{27} \gamma^3 \\ S_{5,2} &= \frac{161032}{81} + \frac{897110}{243} \gamma + \frac{675710}{243} \gamma^2 + \frac{519535}{486} \gamma^3 \\ &+ \frac{101825}{486} \gamma^4 + \frac{4052}{243} \gamma^5 \\ S_{6,0} &\equiv S_6^{(0)} = 5200 + \frac{168830}{27} \gamma + \frac{76805}{27} \gamma^2 \\ &+ \frac{15670}{27} \gamma^3 + \frac{1210}{27} \gamma^4 \\ S_{6,2} &= \frac{11647960}{243} + \frac{8506774}{81} \gamma + \frac{23520634}{243} \gamma^2 + \frac{11712610}{243} \gamma^3 \\ &+ \frac{13297615}{972} \gamma^4 + \frac{169751}{81} \gamma^5 + \frac{14591}{108} \gamma^6 \end{aligned} \quad (63)$$

The results for the variance and S_J for the SSZA for particular values of the spectral index are given in Table 4.

For the *unsmoothed* fields ($\gamma = 0$), analytic results including the two corrective terms beyond the tree-level, were derived by SF97a in the context of the diagrammatic approach. For the variance, skewness, and the kurtosis (the latter only up to the first σ -correction) they give,

$$\sigma^2 \approx \sigma_l^2 + 1.27 \sigma_l^4 + 2.02 \sigma_l^6 + \mathcal{O}(\sigma_{\ddagger}^{\forall})$$

$$S_3 \approx 4 + 4.69 \sigma_l^2 + 13.93 \sigma_l^4 + \mathcal{O}(\sigma_{\ddagger}^6)$$

$$S_4 \approx 30.22 + 98.51 \sigma_l^2 + \mathcal{O}(\sigma_{\ddagger}^{\Delta}). \quad (64)$$

The latter results are to be compared to our results from the SC dynamics in the perturbative regime (truncated at the same order),

$$\sigma^2 \approx \sigma_l^2 + 0.78 \sigma_l^4 + 0.76 \sigma_l^6 + \mathcal{O}(\sigma_{\ddagger}^{\forall})$$

$$S_3 \approx 4 + 4.37 \sigma_l^2 + 9.41 \sigma_l^4 + \mathcal{O}(\sigma_{\ddagger}^{\forall})$$

$$S_4 \approx 30.22 + 92.81 \sigma_l^2 + 331.0 \sigma_l^4 + \mathcal{O}(\sigma_{\ddagger}^{\forall}), \quad (65)$$

which differ by 7 % in the corrective term for S_3 , 6 % in the corrective term for S_4 , and up to 40 % in the one-loop term for the variance. The two-loop contributions for S_3 differ in about 30 % and just give the right order of magnitude for the variance. The two-loop contribution to S_4 ($\sim 331 \sigma_l^2$) must be taken just as an estimate of the actual value for this coefficient in PT, since there are no analytic results available to compare with. All the above quoted differences must be attributed to the tidal effects as argued before what gives further support to the view that the hierarchical amplitudes are essentially of a *shearless* nature unlike the (unreduced) one-point cumulants.

For the smoothed density field in the ZA to the exact PT there is one result available concerning the skewness for $n = -2$ (see S97),

$$S_3 \approx 3 + 0.82 \sigma_l^2 + \mathcal{O}(\sigma_{\ddagger}^{\Delta}), \quad (66)$$

while within the SSZA dynamics, we obtained,

$$S_3 \approx 3 + 0.94 \sigma_l^2 + \mathcal{O}(\sigma_{\ddagger}^{\Delta}), \quad (67)$$

which means a 15% negative contribution from the shear for the first corrective term for that particular value of the spectral index.

In Fig 10 and 11 we display the deviations from the tree-level values for the variance, skewness and kurtosis for the SSZA up to 2nd. and 3rd. order respectively, as we did with the SC dynamics before. In line with the arguments pointed out there, the smoothing effects tend to diminish the non-linear corrections. On the other hand, the lack of a critical index (vanishing non-linearities) for the variance gives further support to our claim that it is due to the local nature of the SC picture and thus, to the loss of the previrialization effect.

6 DISCUSSION AND CONCLUSIONS

No available analytic approximations to the dynamics of cosmological perturbations lead to accurate predictions for the one-point cumulants in the non-linear regime (see §2.8). This applies to popular approximations, such as those based in putting some constraints on any of the fields that couple to the density (such as the FFA or the LPA), the Zel'dovich Approximation (ZA), which puts a constraint on the trajectories of the masses, or the local Lagrangian approximations which assume that the evolution of the density contrast may be described locally, i.e., without any influence of the surrounding matter to the mass trajectory. Despite giving some

SSZA	Unsmoothed		Smoothed	
	$\gamma = 0$	$\gamma = -1$	$\gamma = -2$	$\gamma = -3$
	$n = -3$	$n = -2$	$n = -1$	$n = 0$
$s_{2,4}$	0.78	0.47	0.78	1.69
$s_{2,6}$	0.76	0.13	0.76	5.0
$S_{3,0}$	4	3	2	1
$S_{3,2}$	4.37	0.94	-0.15	-1.13
$S_{3,4}$	9.41	0.37	-0.20	-5.17
$S_{4,0}$	30.22	15.89	6.22	1.22
$S_{4,2}$	92.81	13.85	-0.96	-1.82
$S_{4,4}$	331.0	6.76	-4.75	-3.14
$S_{5,0}$	342.221	122.78	26.67	1.67
$S_{5,2}$	1988.05	200.78	-6.12	-5.31
$S_{5,4}$	10711.3	220.42	46.80	103.38
$S_{6,0}$	5200	1256.11	146.67	2.78
$S_{6,2}$	47933.99	3224.87	-64.03	-27.40
$S_{6,4}$	362136.6	5445.8	-252.77	-2527.2

Table 4. Values for the higher-order perturbative contributions for the SC dynamics in the ZA for the unsmoothed ($n = -3$) and smoothed ($n = -2, -1$) density fields.

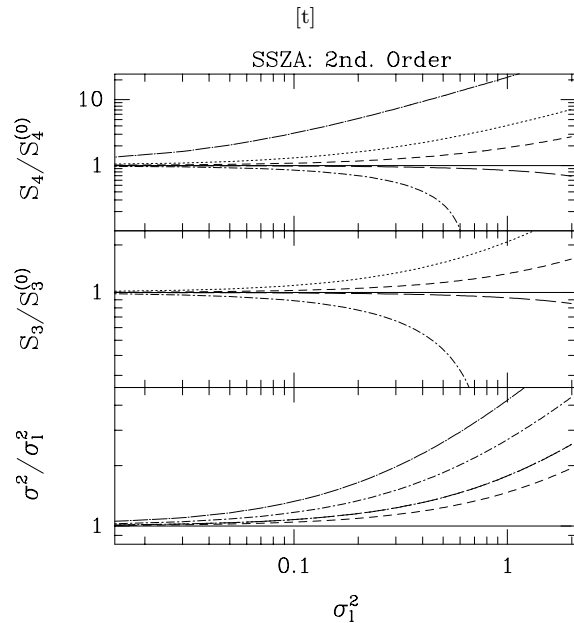


Figure 10. Same as Fig 1, for the SC dynamics in the ZA. In this case, the variance has a minimum corrective term for $n \approx -1$, and the hierarchical amplitudes show a vanishing first corrective term for $n \approx -1.2$. Notice that the $n = 1$ line is not plotted for the skewness since for that particular value the tree-level exactly vanishes.

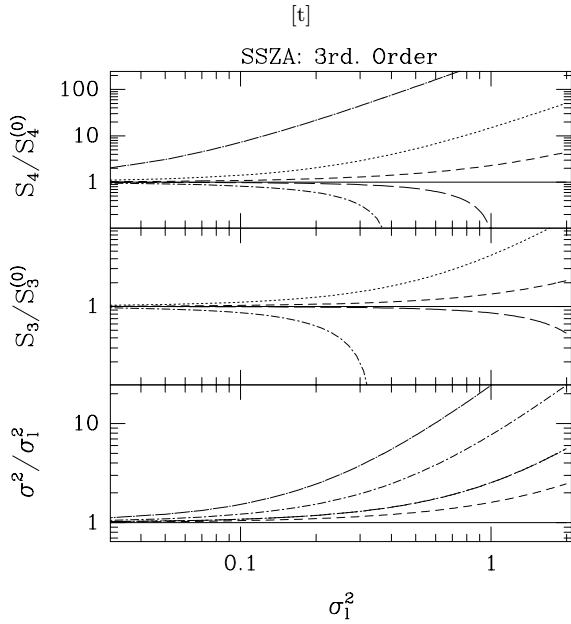


Figure 11. Same as Fig 10, including the 3rd. perturbative order in the analysis.

useful insight to the exact dynamical picture with much simpler calculations, none of them is able to reproduce the exact values for the one-point cumulants even at tree-level as derived in the exact PT.

As mentioned in the introduction there are serious difficulties in applying the exact PT approach to find the evolution of the cumulants of a Gaussian field to higher order (loop) corrections, i.e. to compute next to leading orders. For non-Gaussian initial conditions (NGIC) this problem is apparent even to leading order (in non-linear corrections). An important simplification is found when only the *monopole* or spherical contribution is considered. This contribution is exact for all the tree-graphs. We have shown how the solution in this case can be found directly from the dynamical equations for the evolution of a field (e.g. §3.3 and §5) and is given by the spherical collapse (SC) model for the case of cosmic fluctuations for a non-relativistic pressureless irrotational fluid. This provides with a simpler derivation and interpretation for the results presented by B92, showing why the vertex generating function $\mathcal{G}(-\tau)$ follows the SC model, which lacked a satisfactory explanation in the context of B92.

We have explored the predictions for the one-point cumulants of the density fields in the non-linear regime within the spherical model of collapse. This is done both for the exact dynamics and for the Zel'dovich approximation (see section §5). The SC dynamics, can also be used to study the general case of NGIC (this is done in Paper II), the statistical properties of the velocity and the Ω dependence of these predictions (both shown in Paper III).

A natural shortcoming of the SC model is the loss of *previrialization*, i.e., the generation of large scale random motions induced by the small scale power, which is a non-local phenomenon. This fact is illustrated by the absence of vanishing non-linearities in the variance for a critical index $n_c \approx -1.4$ (see §4.2), which is a direct consequence of *pre-*

virialization, according to the exact PT (SF97b) and found in numerical simulations (Lokas et al. 1995). Despite this, we have shown that the SC model also yields accurate predictions for the cumulants beyond tree-level. Tidal effects in the variance are actually small because the effective index n_{eff} , as measured in galaxy catalogues (such as the APM), is $n_{eff} \simeq [-1, -2]$ (see §4.2) for which either non-linearities are small or tidal effects are subdominant.

For the reduced cumulants S_J , tidal effects seem to cancel out. We find an excellent agreement for the hierarchical amplitudes S_J in the SC perturbative regime with those derived by SF97a for the exact PT in the diagrammatic approach. A similar conclusion follows for the Zel'dovich dynamics (§5), where the monopole approximation results are in good agreement with the exact calculations up to two loops.

We have also compared the predictions for the higher-order moments from the SC model to those measured in CDM and APM-like N-body simulations, and they turned out to be in very good agreement in all cases up to the scales where $\sigma_l \approx 1$, supporting our view that the tidal effects only have a marginal contribution to the reduced cumulants. Furthermore, the break down of the shearless approximation roughly coincides with the regime for which the perturbative approach itself breaks down, $\sigma \simeq 0.5$. That is, where the contribution of the second and the third perturbative order in the SC model are significantly different.

Future work intended to extend the SC model should try to incorporate the local contribution to the tidal field by including other multipoles in the kernels F_n , e.g. including the shear by using the dipole contribution.

ACKNOWLEDGEMENTS

E.G. acknowledges support from CIRIT (Generalitat de Catalunya) grant 1996BEAI300192. This work has been supported by CSIC, DGICYT (Spain), project PB93-0035, and CIRIT, grant GR94-8001.

7 REFERENCES

- Bagla, J.S., Padmanabhan, T., 1994, MNRAS, 266, 227
- Baugh, C.M., Gaztañaga, E., Efstathiou, G., 1995, MNRAS, 274, 1049 (BGE95)
- Bernardeau, F., 1992, ApJ, 392, 1 (B92)
- Bernardeau, F., 1994 A&A 291, 697 (B94a)
- Bernardeau, F., 1994, ApJ, 433, 1 (B94b)
- Bernardeau, F. & Kofman, L., 1994 ApJ, 443, 479
- Bernardeau, F., Singh, T.P., Banerjee, B., Chitre, S.M., 1994, MNRAS, 269, 947
- Bertschinger, E., Jain, B., 1994, ApJ, 431, 486
- Brainerd, T., Scherrer, R.J., Villumsen J. V., 1993, ApJ, 418, 570
- Coles, P., Barrow, J.D., 1987, MNRAS, 228, 407
- Colombi, S., Bernardeau, F., Bouchet, F.R., Hernquist, L., 1996, MNRAS, 287, 241
- Colombi, S., Bouchet, F.R., Hernquist, L., 1996, ApJ, 465, 14 287, 241 10
- Croft, R.A.C., Gaztañaga, E., 1997a, MNRAS, 285, 793

Croft, R.A.C., Gaztañaga, E., 1997b, *ApJ*, in press, astro-ph/9701163

Davis, M., Peebles, P.J.E., 1977, *ApJS*, 34, 425

Fosalba, P., Gaztañaga, E., Elizalde, E., 1997, in preparation.

Fosalba, P., Gaztañaga, E., 1997, in preparation (Paper II).

Fry, J.N., 1984, *ApJ*, 279, 499

Fry, J.N., Gaztañaga, E., 1993, *ApJ*, 413, 447

Gaztañaga, E. & Baugh, C.M., 1995, *MNRAS*, 273, L1

Gaztañaga, E., Fosalba, P., 1997, in preparation (Paper III).

Goroff, M.H., Grinstein, B., Rey, S.J., Wise, M.B., 1986, *ApJ*, 311, 6

Hui, L., Bertschinger, E., 1996, *ApJ*, 471, 1

Jain, B., Bertschinger, E., 1994, *ApJ*, 431, 495

Juszkiewicz, R., Bouchet, F.R., Colombi, S., 1993 *Ap. J. (Letters)*, 412, L9

Kofman, L., Pogosyan, D., 1995, *ApJ*, 442, 30

Lokas, E.L., Juszkiewicz, R., Weinberg, D., Bouchet, F.R., 1995, *MNRAS*, 274, 730

Lokas, E.L., Juszkiewicz, R., Bouchet, F.R., Hivon, E., 1996, *ApJ*, 467, 1

Matarrese S., Lucchin F., Moscardini L., Saez D., 1992 *MNRAS*, 259, 437

Matsubara, T., 1994, *ApJ*, 434, L43

Moutarde, F., Alimi, J.M., Bouchet, F.R., Pellat, R., Raman, A., 1991 *ApJ*, 382, 377

Munshi, D., Sahni, V., Starobinsky, A.A., astro-ph/9402065

Peebles, P.J.E., 1980, *The Large Scale Structure of the Universe*: Princeton University Press, Princeton

Peebles, P.J.E., 1990, *ApJ*, 365, 27

Protogeros, Z.A.M., Melott, A.L., Scherrer, R.J., 1996, 290, 367

Protogeros, Z.A.M., Scherrer, R.J., 1997, *MNRAS*, 284, 425 (PS97)

Scoccimarro, R., 1997, *ApJ*, 487, 1 (S97)

Scoccimarro, R., 1998, *ApJ*, submitted, astro-ph/9711187

Scoccimarro, R., Frieman, J., 1996, *ApJS*, 105, 37 (SF97a)

Scoccimarro, R., Frieman, J., 1996, *ApJ*, 473, 620 (SF97b)

Scoccimarro, R., Colombi, S., Fry, J.N., Frieman, J., Hivon, E., Melott, A., 1997, astro-ph/9704075

Zel'dovich, Ya.B., 1970. *A & A*, 5, 84

APPENDIX A: CUMULANTS FROM THE LOCAL-DENSITY TRANSFORMATION OF GIC IN LAGRANGIAN SPACE

For a generic model of non-linear evolution of the density field in which all the information is encoded in the linear density field alone, one can construct a transformation of the kind,

$$\delta = \mathcal{L}[\delta_1] = \sum_{n=1}^{\infty} \frac{c_n}{n!} [\delta_1]^n \quad (\text{A1})$$

(see Eq.[19] with $c_1 = 1$, to reproduce the linear solution. The latter is what we shall call the *local-density* transformation. If we further assume that the above transformation describes the non-linear evolution in Lagrangian space, it has to be normalized

Next we present the general results for the cumulants including their first non-vanishing perturbative orders for

GIC. For the SC model the calculation corresponds to the process described in §3. Note that this can be extended in a straightforward way to NGIC, just by taking into account the relevant terms to be kept in the perturbation series (see Paper II).

We proceed and give the coefficients of the perturbative terms according to the notation introduced in §4,

$$\begin{aligned}
 s_{2,4} &= 3 - 4c_2 + c_2^2/2 + c_3 \\
 s_{2,6} &= 15 - 36c_2 + 81c_2^2/4 - 3c_2^3/2 + 10c_3 - 7c_2c_3 \\
 &+ 5c_3^2/12 - 7c_4/4 + c_2c_4/2 + c_5/4 \\
 S_{3,0} &= 3c_2 \\
 S_{3,2} &= (-4 + 15c_2^2 - 4c_2^3 - 8c_3 + 3c_4)/2 \\
 S_{3,4} &= -18 + 44c_2 - 16c_2^2 - 3c_2^3 - 7c_2^4 + 5c_2^5/4 \\
 &- 22c_3 + 12c_2c_3 + 10c_2^2c_3 + c_2^3c_3 - 4c_3^2 \\
 &- 7c_2c_3^2/4 + 5c_4 + 9c_2c_4/8 - 9c_2^2c_4/4 \\
 &+ c_3c_4 - 2c_5 + 3c_2c_5/4 + 3c_6/8 \\
 S_{4,0} &= 12c_2^2 + 4c_3 \\
 S_{4,2} &= 6 - 36c_2 + 15c_2^2 + 60c_2^3 - 15c_2^4 - 4c_3 \\
 &- 20c_2c_3 - 6c_2^2c_3 - 5c_4 + 18c_2c_4 + 2c_5 \\
 S_{4,4} &= (180 - 984c_2 + 1488c_2^2 - 534c_2^3 + 99c_2^4 \\
 &- 180c_2^5 + 27c_2^6 + 260c_3 - 816c_2c_3 \\
 &+ 232c_2^2c_3 + 144c_2^3c_3 + 30c_2^4c_3 + 76c_3^2 \\
 &- 48c_2c_3^2 - 30c_2^2c_3^2 - 4c_3^3 - 86c_4 \\
 &+ 163c_2c_4 + 129c_2^2c_4 - 66c_2^3c_4 - 72c_3c_4 \\
 &+ 8c_2c_3c_4 + 16c_4^2 + 8c_5 - 40c_2c_5 \\
 &+ 12c_2^2c_5 + 7c_3c_5 - 5c_6 + 12c_2c_6 + c_7)/2 \\
 S_{5,0} &= 60c_2^3 + 60c_2c_3 + 5c_4 \\
 S_{5,2} &= -24 + 180c_2 - 510c_2^2 + 240c_2^3 + 450c_2^4 \\
 &- 108c_2^5 - 80c_3 + 90c_2^2c_3 - 120c_2^3c_3 \\
 &- 90c_3^2 - 10c_4 - 105c_2c_4/2 + 170c_2^2c_4 \\
 &+ 50c_3c_4 - 6c_5 + 40c_2c_5 + 5c_6/2 \\
 S_{6,0} &= 6(60c_2^4 + 120c_2^2c_3 + 15c_3^2 + 20c_2c_4 + c_5) \\
 S_{6,2} &= 120 - 1080c_2 + 3870c_2^2 - 6930c_2^3 + 3060c_2^4 \\
 &+ 3600c_2^5 - 840c_2^6 + 480c_3 - 3240c_2c_3 \\
 &+ 1500c_2^2c_3 + 3840c_2^3c_3 - 1800c_2^4c_3 \\
 &- 110c_3^2 - 1620c_2c_3^2 - 225c_2^2c_3^2 + 30c_3^3 \\
 &- 150c_4 - 135c_2c_4 - 60c_2^2c_4 + 1500c_2^3c_4 \\
 &- 420c_3c_4 + 1500c_2c_3c_4 + 105c_4^2 - 18c_5 \\
 &- 108c_2c_5 + 585c_2^2c_5 + 135c_3c_5 - 7c_6 \\
 &+ 75c_2c_6 + 3c_7. \quad (\text{A2})
 \end{aligned}$$

Note that all the values of c_n can be obtained or can be expressed in terms of the tree-level alone: $S_{J,0}$, indicating that the knowledge of the tree level is enough to fully specify the undelaying local-density transformation, and therefore to generate all higher order corrections.

Furthermore, we can make use of the general formula for the top-hat filtering derived in §3.4, and generalize the above given expressions by replacing the unsmoothed c_k coefficients by their smoothed counterparts \bar{c}_k in the following way:

$$\begin{aligned}
 \bar{c}_2 &= c_2 + \frac{\gamma_1}{3} \\
 \bar{c}_3 &= c_3 + \frac{\gamma_1}{2} - \frac{3}{2} c_2 \gamma_1 + \frac{\gamma_1^2}{4} + \frac{\gamma_2}{6} \\
 \bar{c}_4 &= c_4 + \frac{4}{3} \gamma_1 - 4 c_2 \gamma_1 + 2 c_2^2 \gamma_1 + \frac{8}{3} c_3 \gamma_1 \\
 &- \frac{4}{3} \gamma_1^2 + \frac{8}{3} c_2 \gamma_1^2 + \frac{8}{27} \gamma_1^3 - \frac{2}{3} \gamma_2 + \frac{4}{3} c_2 \gamma_2 \\
 &+ \frac{4}{9} \gamma_1 \gamma_2 + \frac{2}{27} \gamma_3,
 \end{aligned} \tag{A3}$$

and so on, where:

$$\gamma_p = \gamma_p(R) = \frac{d^p \log \hat{\sigma}_l^2}{d \log^p R}.$$

The latter expressions are valid for arbitrary dynamics (to be specified through the unsmoothed coefficients) and a generic initial power spectrum.

This expressions can be used for the particular cases of interest. For the SC dynamics ($c_k = \nu_k$ as given by Eq.[34]) we find for the first coefficients of the cumulants,

$$\begin{aligned}
 s_{2,4} &= \frac{909}{1323} + \frac{143}{126} \gamma_1 + \frac{11}{36} \gamma_1^2 + \frac{\gamma_2}{6} \\
 S_{3,0} &= \frac{34}{7} + \gamma_1 \\
 S_{3,2} &= \frac{1026488}{101871} + \frac{12862}{1323} \gamma_1 + \frac{407}{126} \gamma_1^2 + \frac{10}{27} \gamma_1^3 \\
 &+ \frac{11}{7} \gamma_2 + \frac{2}{3} \gamma_1 \gamma_2 + \frac{\gamma_3}{9} \\
 S_{4,0} &= \frac{60712}{1323} + \frac{62}{3} \gamma_1 + \frac{7}{3} \gamma_1^2 + \frac{2}{3} \gamma_2 \\
 S_{4,2} &= \frac{22336534498}{83432349} + \frac{42649448}{130977} \gamma_1 + \frac{3571621}{23814} \gamma_1^2 \\
 &+ \frac{35047}{1134} \gamma_1^3 + \frac{1549}{648} \gamma_1^4 + \frac{575777}{11907} \gamma_2 + \frac{5981}{189} \gamma_1 \gamma_2 \\
 &+ \frac{263}{54} \gamma_1^2 \gamma_2 + \frac{25}{54} \gamma_2^2 + \frac{2084}{567} \gamma_3 \\
 &+ \frac{86}{81} \gamma_1 \gamma_3 + \frac{5}{81} \gamma_4.
 \end{aligned} \tag{A4}$$

This way, the results for the SC and SSZA dynamics described in the text (see §4 and §5 respectively) are given as particular cases of this *local-density* transformation in Lagrangian space whenever we replace the c_k coefficients by those associated to the relevant dynamics: $c_k = \nu_k$ or $c_k = \bar{\nu}_k$ for the unsmoothed or smoothed fields respectively (the previous being a particular case of the latter). The same expressions hold for the velocity fields replacing $c_k = \mu_k$ or $c_k = \bar{\mu}_k$ for the unsmoothed and smoothed fields respectively. These μ_k coefficients are related to those for the density field through the equation of continuity (see Paper III for details).

APPENDIX B: CUMULANTS FROM THE LOCAL-DENSITY TRANSFORMATION OF GIC IN EULER SPACE

In this section we derive the cumulants from the local-density transformation in Euler space to quantify the departures from the Lagrangian formulation and give values

SC	Unsmoothed				Smoothed			
	$\gamma = 0$	$\gamma = -1$	$\gamma = -2$	$\gamma = -3$	$n = -3$	$n = -2$	$n = -1$	$n = 0$
$s_{2,4}$	4.92	2.76	1.20	0.26				
$s_{2,6}$	22.49	4.99	0.37	0.003				
$S_{3,0}$	4.86	3.86	2.86	1.86				
$S_{3,2}$	54.64	21.80	5.68	0.38				
$S_{4,0}$	45.89	27.56	13.89	4.89				
$S_{4,2}$	418.14	74.17	3.45	0.02				

Table B1. Estimates of the cumulants in the SC model in Euler space.

for the SC dynamics. The formulae given below reproduce those given in FG93. There, they were presented as a bias transformation between the visible and the underlying matter fluctuations.

The first perturbative contributions to the cumulants in Euler space are the following,

$$\begin{aligned}
 s_{2,4} &= c_2^2/2 + c_3 \\
 S_{3,0} &= 3c_2 \\
 S_{3,2} &= c_2^3 + 6c_2 c_3 + 3c_4/2 \\
 S_{4,0} &= 12c_2^2 + 4c_3 \\
 S_{4,2} &= -15c_2^4 - 6c_2^2 c_3 + 18c_2 c_4 + 2c_5.
 \end{aligned} \tag{B1}$$

Replacing in these expressions the values for the SC dynamics with a top-hat filter and a power-law spectrum, i.e., introducing the smoothed coefficients given by Eqs.[48],[34], we get estimates for the cumulants as summarized in Table B1.

Notice that unlike the case for the SC estimates from Lagrangian space, the Euler estimates just give the right order of magnitude for the cumulants when compared against exact analytic calculations (see Eqs.[54], [56]).

APPENDIX C: TOP-HAT SMOOTHING IN FOURIER SPACE

To illustrate the fact that the SC model gives the correct smoothed tree-level amplitudes for GIC for a top-hat window, we shall derive $\bar{\nu}_2$ explicitly by imposing the SC hypothesis in Fourier space and show that the skewness $S_3 = 3\bar{\nu}_2$, exactly reproduces the leading order exact perturbative result (48): e.g. $\bar{\nu}_2 = \nu_2 + \gamma/3$. We perform the calculation in Euler space but the result does not differ from that in Lagrangian space at tree-level for Gaussian initial conditions, as mentioned in (38), which only contributes to higher perturbative orders (σ -corrections).

To see this, we recall the properties derived by Bernardeau 1994b (B94b) for a top-hat window function (spherical window) defined as,

$$W_{TH}(\mathbf{x}) = 1 \quad \text{if } |\mathbf{x}| \leq R_0,$$

and 0 otherwise, for a scale R_0 , so that the smoothed fields are obtained through the integral,

$$\bar{\delta} \equiv \delta(R_0) = \int d^3\mathbf{x} W_{TH}(\mathbf{x})\delta(\mathbf{x}),$$

We turn to Fourier space for convenience, where the smoothed fields are expressed as,

$$\delta(R_0) = \int \frac{d^3\mathbf{k}}{(2\pi)^{3/2}} W_{TH}(\mathbf{k}R_0)\delta(k),$$

where $W_{TH}(\mathbf{k}R_0)$ is the Fourier transform of $W_{TH}(\mathbf{x})$. In particular, for the second-order in the perturbative series, we have for the smoothed field

$$\delta_2(R_0) = \int \frac{d^3\mathbf{k}_1}{(2\pi)^{3/2}} \frac{d^3\mathbf{k}_2}{(2\pi)^{3/2}} \delta_{k_1} \delta_{k_2} W(|\mathbf{k}_1 + \mathbf{k}_2| R_0) \times \left[D_1^2 \left(P_{1,2} - \frac{3}{2} Q_{1,2} \right) + \frac{3}{4} D_2 Q_{1,2} \right],$$

where,

$$P_{1,2} = 1 + \frac{\mathbf{k}_1 \cdot \mathbf{k}_2}{k_1^2 k_2^2}, \quad Q_{1,2} = 1 + \frac{(\mathbf{k}_1 \cdot \mathbf{k}_2)^2}{k_1^2 k_2^2},$$

and D_i are the time-dependent factors for the i th-perturbative order to be solved with the SC equations of motion. Now, decomposing the integrals in its angular and radial part and translating the property of spherical symmetry into Fourier space language, condition,

$$\delta_{k_i} = \delta_{|k_i|}, \quad (C1)$$

we can apply the properties for the top-hat window function (see B94b, eqs.[A5] and [A6]) and get,

$$\delta_2(R_0) = \left(\frac{D_2}{2 D_1^2} + \frac{1}{6} \frac{d \log[\delta_l(R_0)]^2}{d \log R_0} \right) [\delta_l(R_0)]^2,$$

since,

$$\delta_l(R_0) = \int \frac{d^3\mathbf{k}}{(2\pi)^{3/2}} W_{TH}(\mathbf{k}R_0)\delta_k D_1(t).$$

We further use the fact that in general [see 41)] the smoothed linear density contrast at a point x , can be factorized in its scale dependent part $\sigma(R_0)$ and its normalized linear field $\varepsilon(x)$,

$$\delta_l(R_0) \equiv \delta_l(R_0, x) = \sigma_l(R_0) \eta(x) \quad (C2)$$

and we finally get:

$$\delta_2(R_0) = \frac{1}{2} \left(\frac{34}{21} + \frac{1}{3} \frac{d \log[\sigma_l(R_0)]^2}{d \log R_0} \right) [\delta_l(R_0)]^2. \quad (C3)$$

If we define:

$$\delta_2(R_0) \equiv \frac{\bar{\nu}_2}{2} [\delta_l(R_0)]^2 \quad (C4)$$

we find

$$\bar{\nu}_2 = \frac{34}{21} + \frac{1}{3} \frac{d \log[\sigma_l(R_0)]^2}{d \log R_0} = \nu_2 + \gamma/3 \quad (C5)$$

which exactly reproduces Eq.[48]. This result can be extended to higher orders following the properties of the top hat presented by B94b.